Atmos. Chem. Phys., 12, 4743–4774, 2012
www.atmos-chem-phys.net/12/4743/2012/
doi:10.5194/acp-12-4743-2012

Atmospheric Chemistry and Physics

Global modeling of SOA formation from dicarbonyls, epoxides, organic nitrates and peroxides

G. Lin[1], J. E. Penner[1], S. Sillman[1], D. Taraborrelli[2], and J. Lelieveld[2,3]

[1]Department of Atmospheric, Oceanic, and Space Sciences, University of Michigan, Ann Arbor, Michigan, USA
[2]Department of Atmospheric Chemistry, Max Planck Institute for Chemistry, Mainz, Germany
[3]The Cyprus Institute, Nicosia, Cyprus

Correspondence to: G. Lin (gxlin@umich.edu)

Received: 5 August 2011 – Published in Atmos. Chem. Phys. Discuss.: 22 September 2011
Revised: 2 April 2012 – Accepted: 19 April 2012 – Published: 31 May 2012

Abstract. Recent experimental findings indicate that secondary organic aerosol (SOA) represents an important and, under many circumstances, the major fraction of the organic aerosol burden. Here, we use a global 3-D model (IMPACT) to test the results of different mechanisms for the production of SOA. The basic mechanism includes SOA formation from organic nitrates and peroxides produced from an explicit chemical formulation, using partition coefficients based on thermodynamic principles together with assumptions for the rate of formation of low-volatility oligomers. We also include the formation of low-volatility SOA from the reaction of glyoxal and methylglyoxal on aqueous aerosols and cloud droplets as well as from the reaction of epoxides on aqueous aerosols. A model simulation including these SOA formation mechanisms gives an annual global SOA production of 120.5 Tg. The global production of SOA is decreased substantially to 90.8 Tg yr^{-1} if the HO_x regeneration mechanism proposed by Peeters et al. (2009) is used. Model predictions with and without this HO_x (OH and HO_2) regeneration scheme are compared with multiple surface observation datasets, namely: the Interagency Monitoring of Protected Visual Environments (IMPROVE) for the United States, the European Monitoring and Evaluation Programme (EMEP), and aerosol mass spectrometry (AMS) data measured in both the Northern Hemisphere and tropical forest regions. All model simulations show reasonable agreement with the organic carbon mass observed in the IMPROVE network and the AMS dataset, however observations in Europe are significantly underestimated, which may be caused by an underestimation of primary organic aerosol emissions (POA) in winter and of emissions and/or SOA production in the summer. The modeled organic aerosol concentrations tend to be higher by roughly a factor of three when compared with measurements at three tropical forest sites. This overestimate suggests that more measurements and model studies are needed to examine the formation of organic aerosols in the tropics. The modeled organic carbon (OC) in the free troposphere is in agreement with measurements in the ITCT-2K4 aircraft campaign over North America and in pollution layers off Asia during the INTEX-B campaign, although the model underestimates OC in the free troposphere in comparison with the ACE-Asia campaign off the coast of Japan.

1 Introduction

Atmospheric particles have important impacts on human health, air quality as well as regional and global climate and climate change. Organic aerosols represent a large fraction of the particulate mass at both urban and remote locations (Kanakidou et al., 2005; Zhang et al., 2007; Jimenez et al., 2009). They are often categorized as either "primary organic aerosol (POA)", a class of organic compounds that is emitted directly into the atmosphere in particulate form, or "secondary organic aerosols (SOA)", which are formed by atmospheric oxidation of volatile organic compounds (VOCs). The distinction between these two categories, however, is changing as a result of recent studies which show that the volatility of emitted particles can change as a result of the oxidation of primary emissions, which can subsequently provide an extra source of SOA (Robinson et al., 2007). Previously unrecognized low-volatility compounds

(LV-OOA) are also present in measured SOA (Jimenez et al., 2009).

Despite the importance of organic aerosols (OA) in the environment, data sets to constrain models are limited. Nevertheless, based on available data sets it appears that models tend to underestimate SOA concentrations in the boundary layer (e.g., Johnson et al., 2006; Volkamer et al., 2006; Kleinman et al., 2008; Simpson et al., 2007) as well as in the free troposphere (Heald et at., 2005). Johnson et al. (2006) studied SOA formation in the UK using a fully explicit chemical scheme in the modified Master Chemical Mechanism (MCM v3.1), and found that they had to increase all partitioning coefficients of SOA precursors by a factor of 500 in order to capture observed OA levels. Volkamer et al. (2006) employed aerosol mass spectrometer (AMS) measurements to analyze the surface concentrations of oxidized organic aerosol (OOA) in Mexico City. The measured SOA was about 8 times larger than a conservative (high end) estimate from an SOA model based on an empirical parameterization of chamber experiments. Their results were corroborated by Kleinman et al. (2008) who reported a discrepancy of an order of magnitude between the measured SOA taken in aircraft data from the MILAGRO 2006 campaign and that computed by a model. Simpson et al. (2007) found that their SOA modeling framework under-predicted SOA concentrations at Southern European sites, but predicted SOA levels that were within the range of observations in Northern Europe. Heald et al. (2005) compared free tropospheric OA measurements from the Asia Pacific Regional Aerosol Characterization Experiment (ACE-Asia) field campaign with predictions from the global chemical transport model GEOS-Chem and concluded that a significant source of SOA was missing in the free troposphere.

Although these regional and global models showed a tendency to under-predict organic carbon (OC) concentrations in polluted regions, there is no universal underestimation for regions in which biogenic sources dominate (Capes et al., 2009; Chen et al., 2009; Slowik et al., 2010). Capes et al. (2009) presented measurements of OA over subtropical West Africa during the wet season using data from the UK Facility for Airborne Atmospheric Measurements (FAAM) aircraft. Their theoretical SOA estimates, which were based on smog-chamber aerosol yields together with estimates of the amount of isoprene and monoterpenes present at their site, under-represented the measured organic matter (OM) by about a factor of 4. Chen et al. (2009) presented loadings of organic aerosols using the GEOS-Chem model that were 35 % lower than measurements in the Amazon Basin taken using a high-resolution AMS during the wet season of 2008. In contrast, Slowik et al. (2010) obtained very good agreement between measurements in an eastern Canadian forest region and simulations using a regional air quality model.

The reasons for the differences between measured vs. modeled SOA in different regions remain unclear due to the numerous and complex chemical and physical phenomena involved in SOA formation (Hallquist et al., 2009; Pankow and Barsanti, 2009). One major uncertainty relates to the formation of gaseous secondary organics. It has been estimated that there are many hundreds of thousands of different organic compounds in the atmosphere (Goldstein and Galbally, 2007), with each compound further undergoing a number of atmospheric reactions to produce a range of oxidized products (Hallquist et al., 2009). Therefore, the atmosphere contains a highly complex mixture with a myriad of structurally different organic oxygenates having a wide range of physicochemical properties and different gas-to-particle-transfer potentials (Utembe et al., 2011; Lee-Talor et al., 2011). The complexity of the emitted VOC mixture and the oxidation chemistry requires a rigorous and thorough gas-phase chemical mechanism that describes SOA formation. Donahue et al. (2009) argues that the complexity of SOA cannot be followed in detail and requires an approach where species are lumped into individual "volatility basis sets". Although the development of a "rigorous" mechanism may not be completely possible given that there are many species and reactions that we still do not know, we prefer to tie the formation of SOA to an explicit chemical mechanism, so that the contribution of the specific reaction mechanism and the specific individual species to SOA formation is known. Without this, it may not be possible to compare specific species with measurements (though, admittedly few are available now). Also, we think this approach can be easily updated as chemical mechanisms are further developed. Isoprene emissions ($\sim$500 Tg C yr^{-1}) (Guenther et al., 2006) constitute around one third of total VOC emissions to the atmosphere (Goldstein and Galbally, 2007). In addition, SOA derived from biogenic VOCs dominate model-predicted global atmospheric SOA burdens (Tsigaridis et al., 2006; Henze et al., 2008) and many measured data also suggest that most of the SOA is associated with biogenic emissions (Lewis et al, 2004; Kleindienst et al, 2007; Szidat et al., 2009; Goldstein et al., 2009). However, the precise mechanisms of the SOA formation are not known. Further, field studies in forested environments have found much higher hydroxyl (OH) radical concentrations than those predicted by models that are based on traditional mechanisms in which isoprene peroxy radicals react mainly with HO_2 to form hydroperoxides in low NO_x conditions (Lelieveld et al., 2008; Pugh et al., 2010). This indicates that the isoprene oxidation mechanisms traditionally used in chemistry-transport models may require substantial revision.

In addition to the oxidation mechanisms for VOCs, other efforts have focused on the gap between measured and modeled SOA. The non-volatile primary organic aerosol (POA) from diesel exhaust and biomass burning is known to include low-volatility compounds that partition between the gas and aerosol phase. These can then undergo gas-phase oxidation to form species of different volatilities that form SOA (Robinson et al., 2007; Huffman et al., 2009). This previously neglected SOA source has been explored using box (Dzepina et al., 2009), regional (Hodzic et al., 2010) and

global (Pye and Seinfeld, 2010) models, which indicate that this may be an important source of SOA. These studies show that adding this new SOA source can bring the model simulation into better agreement with the observations in Mexico City (Li et al., 2011), or can even over-predict the observations (Dzepina et al., 2011; Hodzic et al., 2010). However, there is still substantial uncertainty in the emissions, reaction rates, and SOA yields of the traditional primary emitted aerosols (Pye and Seinfeld, 2010; Spracklen et al., 2011).

The propensity of VOC oxidation products to undergo further reactions within or on the condensed phase has also been established as playing a key role in the formation and growth of SOA over the last 5–10 yr. Condensed-phase reactions can cause the vapor pressure of organics to be lowered by several orders of magnitude, either by oxidation or formation of high-molecular-weight species (e.g., through oligomerization) (Hallquist et al., 2009). The rate of formation of these low volatile compounds increases in the presence of inorganic acid seed aerosol, at least for the products formed in the ozonolysis of alpha-pinene (Jang et al., 2006; Czoschke et al., 2003; Iinuma et al., 2004; Gao et al., 2004a, b). Additionally, in regions where isoprene is present under low NO_x conditions, epoxydiols can form (Paulot et al., 2009) and their reactive uptake on acidic sulphate aerosols (Minerath and Elrod, 2009) may lead to a 20-fold increase in OA mass yields from isoprene (Surratt et al., 2010). Similarly, the uptake of gas-phase glyoxal into aqueous ammonium sulfate particles has been observed (Jang and Kamens, 2001; Hastings et al., 2005; Kroll et al., 2005b; Liggio et al., 2005a). Following these observations, the production of SOA by reactive uptake of glyoxal as well as methylglyoxal was examined in a global model (Fu et al., 2008).

In this paper, we begin with a short description of the model in Sect. 2, followed by a description of the gas-phase chemical mechanisms for the oxidation of VOCs and the formation of SOA from gas-particle partitioning of semivolatile organic compounds (SVOCs). We describe our treatment for the formation of low-volatility or oligomeric compounds, and for irreversible uptake of glyoxal, methylglyoxal and epoxydiols. Our model results using different chemical mechanisms for HO_x (OH and HO_2) recycling are presented in Sect. 3. Section 4 compares our results with both surface and free tropospheric observations, followed by sensitivity tests in which we vary the oligomer formation rate in Sect. 5. A summary is presented in Sect. 6.

2 Model description

Here, we use the Integrated Massively Parallel Atmospheric Chemical Transport (IMPACT) model that was developed at the Lawrence Livermore National Laboratory (LLNL) (Rotman et al., 2004) and at the University of Michigan (Penner et al., 1998; Liu and Penner, 2002; Liu et al., 2005; Ito et al., 2007). The IMPACT model was developed using massively parallel computer architecture and was extended by Liu and Penner (2002) to treat the mass of sulfate aerosol as a prognostic variable. It was further extended by Liu et al. (2005) to treat the microphysics of sulfate aerosol and the interactions between sulfate and non-sulfate aerosols based on the aerosol module developed by Herzog et al. (2004). Ito et al. (2007) investigated the effect of non-methane volatile organic compounds on tropospheric ozone and its precursors using the IMPACT model, with a modified numerical solution for photochemistry (Sillman, 1991) and a modified chemical mechanism (Ito et al., 2007). In this paper, we used the same microphysics module described in Liu et al. (2005). We prescribed the SOA size distribution to be the same as that for biomass burning OM in Liu et al. (2005), but allowed it to interact with sulfate through condensation of sulfuric acid, through coagulation with pure sulfate aerosols, and through aqueous formation of sulfate. We use the 1997 meteorological fields from the National Aeronautics and Space Administration (NASA) Data Assimilation Office (DAO) GEOS-START (Goddard EOS Assimilation System-Stratospheric Tracers of Atmospheric Transport) model (Coy and Swinbank, 1997; Coy et al., 1997). The meteorology was defined on a 4° latitude × 5° longitude horizontal grids with 46 vertical layers. The model was run for a 1-yr time period with a 1-month spin up time.

2.1 Atmospheric oxidation mechanisms for SOA precursors

2.1.1 Chemical mechanism by Ito et al. (2007)

We used the chemical mechanism published by Ito et al. (2007) to represent the basic photochemistry of O_3, OH, NO_x and volatile organic compounds (VOC). The Ito et al. (2007) mechanism uses surrogate species to represent classes of VOC, so that (for example) the chemistry of toluene is also used to represent ethyl benzene. Representation of the chemical reaction pathways to form SOA described below, are all incorporated in the Ito et al. (2007) gas-phase mechanism. In certain cases we have used modified reaction sequences (e.g., Peeters et al. (2009) for the first stages of isoprene oxidation) as replacements for the original sequences from Ito et al. (2007). In these cases the subsequent reaction products (e.g., methylvinyl ketone) react as in Ito et al. (2007), unless otherwise specified. The gas-phase oxidation is initiated by reaction with hydroxyl (OH) radicals, O_3, nitrate (NO_3) radicals or via photolysis, leading to the formation of organic peroxy radicals (RO_2). In the presence of nitrogen oxides ($NO_x = NO + NO_2$), RO_2, oxy radicals (RO) and the hydroperoxy radical (HO_2) can act as chain propagating species, leading to the regeneration of OH (e.g., Kroll and Seinfeld, 2008). The reactions of RO_2 and HO_2 with NO play a key role in these catalytic cycles, since the

associated oxidation of NO to NO_2 leads to the formation of ozone by the subsequent photolysis of NO_2:

$$RO_2 + NO \rightarrow RO + NO_2 \quad \text{(R1)}$$

$$HO_2 + NO \rightarrow OH + NO_2 \quad \text{(R2)}$$

At low levels of NO_x, RO_2 will instead react with HO_2 and then form a hydroperoxide, leading to a general suppression of the concentrations of the free radical species:

$$RO_2 + HO_2 \rightarrow ROOH + O_2\ . \quad \text{(R3)}$$

2.1.2 Epoxide formation following Paulot et al. (2009)

The gas-phase formation of epoxides (IEPOX) has been characterized by Paulot et al. (2009). These compounds are formed in the OH-initiated oxidation of isoprene hydroperoxide (RIP) under low-NO_x conditions. IEPOX formation is accompanied by OH regeneration and is implemented in the model as shown below:

$$RIP + OH \rightarrow IEPOX + OH \quad \text{(R4)}$$

The subsequent oxidation of IEPOX is as follows:

$$IEPOX + OH \rightarrow IEPOXO2 \quad \text{(R5)}$$

$$\begin{aligned} IEPOX + NO \rightarrow\ & NO_2 + 0.725\,HAC + 0.275\,GLYC + \\ & 0.275\,GLYX + 0.275\,MGLY + 0.375\,HCHO + \\ & 0.074\,ACO2 + 0.251\,CO \end{aligned} \quad \text{(R6)}$$

$$\begin{aligned} IEPOX + HO_2 \leftarrow\ & 0.825\,HO_2 + 0.125\,OH + 0.725\,HAC + \\ & 0.275\,GLYC + 0.275\,GLYX + 0.275\,MGLY + \\ & 0.375\,HCHO + 0.074\,ACO2 + 0.251\,CO \end{aligned} \quad \text{(R7)}$$

The short names used here (e.g., HAC) are adopted from Ito et al. (2007). The full species and chemical formulas can be found in Table S2 in the Supplement.

2.1.3 HO_x regeneration in isoprene oxidation

As described in the Introduction, analysis of recent direct measurements of HO_x (OH and HO_2) over the Amazonian rainforest (Lelieveld et al., 2008) and the tropical forests of Borneo (Pugh et al., 2010) showed that the traditional chemistry used in numerical model studies cannot explain the high measured OH concentrations, which suggested that there is a yet unknown recycling mechanism for OH. To address this, Peeters et al. (2009) proposed and theoretically quantified a novel HO_x-regenerating pathway for the OH-initiated oxidation of isoprene. This oxidation mechanism has the following main features. The isoprene hydroxyl alkyl radicals first react with O_2 to form three isoprene peroxyradicals, which are in near-equilibrium steady-state. Some of the isoprene peroxy radicals, i.e., β-peroxys, are proposed to undergo 1,5-H shifts that compete with the conventional reaction channels through HO_2, RO_2 and NO, leading to OH and HCHO along with either methacrolein (MACR) or methylvinylketone (MVK). Similarly, the Z-δ-OH-peroxys may undergo fast 1,6-H shifts that lead to the formation of HO_2 and hydroperoxy aldehydes, which can rapidly photo-dissociate, initiating a reaction cascade that can yield 1–3 OH radicals. Our simplified representation of the HO_x recycling mechanism is detailed in Table S3 in the Supplement.

Although the chemical mechanism framework proposed by Peeters et al. (2009) provides a significant potential for addressing the atmospheric OH recycling issue, some atmospheric field measurements (e.g., Karl et al., 2009) and laboratory data (e.g., Paulot et al. 2009) indicate that it does not fully capture all observations. Karl et al. (2009) pointed out that the Peeters et al. (2009) mechanism overestimates MVK/MACR ratios and under-predicts the sum of MVK and MACR relative to isoprene when compared to field measurements conducted during the Amazonian Aerosol Characterization Experiment (AMAZE-08). Unrealistically high ratios of MVK/MACR and peroxyacetyl nitrate (PAN)/peroxymethacryloyl nitrate (MPAN) were also reported by Archibald et al. (2010) using the Peeters et al. (2009) mechanism. In addition, Paulot et al. (2009) carried out a chamber experiment and found a lower yield ($<10\,\%$) for the formation of the hydroperoxy-methylbutenal isomers (HPC41CHO and HPC42CHO) than that proposed by Peeters et al. (2009). Moreover, Da Silva et al. (2010) used density functional theory (DFT) methods to calculate the 1,5-H atom shift isomerization rates for the isoprene-derived β-peroxy radicals and obtained an order of magnitude lower rates than those reported by Peeters et al. (2009). To reconcile the differences between Peeters et al. (2009) and the atmospheric observations or laboratory data mentioned above, both Karl et al. (2009) and Archibald et al. (2010) decreased the 1,5-H shift, 1,6-H shift rates by a factor of 10 as a sensitivity test. However, Peeters and Müller (2010) showed that Paulot et al. (2009) did not account for 25 % of the isoprene peroxy radicals produced during the experiments. During the preparation of this manuscript, an experimental estimate for 1,6-H shift was published (Crounse et al., 2011) and was a factor of 50 ± 25 lower than the estimate of Peeters and Müller (2010). In this paper, we carried out three different simulations with different gas-phase chemical mechanisms (see Table 1). Simulation A only employs the Ito et al. (2007) chemical mechanism together with the epoxide formation mechanism from Paulot et al. (2009). Simulation B includes the HO_x recycling mechanism during isoprene oxidation from Peeters et al. (2009) and the mechanism in Simulation A with some reactions modified in accordance with the recent literature (Table S4 in the Supplement). Simulation C uses the same chemical mechanism as Simulation B, but with the 1,5-H and 1,6-H shift rates reduced by a factor 10.

Table 1. Description of three runs and five SOA components performed in this paper.

Name of runs or SOA components	Description
Simulation A	Bases on Ito et al. (2007) chemistry mechanism and epoxide formation from isoprene from Paulot et al. (2009), without HO_x recycling. It uses emissions for year 2000, and meteorology for 1997.
Simulation B	Includes the mechanism in Simulation A with some reactions modified in accord with the recent literature and HO_x regeneration through isoprene oxidation proposed by Peeters et al. (2009).
Simulation C	The same chemistry mechanism as Simulation B, but with a reduced rate for the 1,5-H and 1,6-H shifts in isoprene radicals by a factor of 10.
sv_oSOA	SOA formed from the traditional gas-particle partitioning of SVOCs produced by oxidation of VOCs. There are 23 SVOC species in Simulation A, and 26 SVOC species in Simulation B and C (see the Table S1).
ne_oSOA	Low-volatility SOA formed from irreversible aerosol-phase reactions of sv_oSOA (i.e., oligomer formation), assuming a fixed lifetime for the oligomer formation.
ne_GLYX	Glyoxal SOA formed from the irreversible uptake of gas-phase glyoxal into aqueous sulfate and clouds following the methods used in Fu et al. (2008, 2009).
ne_MGLY	Methylglyoxal SOA formed from the irreversible uptake of gas-phase methylglyoxal into aqueous sulfate and clouds following the methods used in Fu et al. (2008, 2009).
ne_IEPOX	Epoxide SOA formed from the irreversible uptake of gas-phase epoxide into aqueous sulfate aerosol with the same uptake coefficient as glyoxal and methylglyoxal.

2.2 SOA formation

2.2.1 Gas-particle partitioning of semi-volatile organic compounds

Traditionally, SOA is thought to be formed from gas-particle partitioning of semi-volatile organic compounds which are derived from the oxidation of VOCs. The gas-particle partitioning of organics produced during gas-phase oxidation is based on the absorptive model described by Pankow (1994), which assumes thermodynamic equilibrium between the gas and particulate phase. According to this model, partitioning of each semi-volatile organic compound between the gas and aerosol phases can be described by an equilibrium partitioning coefficient K_i ($m^3\,\mu g^{-1}$), or equivalently, its inverse, the effective saturation vapor concentration, C_i^* ($\mu g\,m^{-3}$), (Donahue et al., 2006),

$$\frac{[A_i]}{[G_i]} = K_i C_{OM} = \frac{C_{OM}}{C_i^*} \quad (1)$$

where C_{OM} ($\mu g\,m^{-3}$) is the mass concentration per unit volume of air of the total absorbing particle phase, which may include the pre-existing organic aerosol into which semi-volatile organics partition and possibly the aqueous portion of the organics if the semi-volatile organics are water-soluble; $[A_i]$ ($\mu g\,m^{-3}$) and $[G_i]$ ($\mu g\,m^{-3}$) are the concentrations of species i in the aerosol and gas phases, respectively. Here, we define

$$C_{OM} = [POA] + \sum_{i=1}^{n} [A_i]\,. \quad (2)$$

In this equation n is the number of species that can partition to the aerosol phase; [POA] ($\mu g\,m^{-3}$) is the concentration of primary organic aerosols, though the inclusion of the hydrophobic un-oxidized POA in the estimate of [POA] may tend to overestimate the yield of SOA (Song et al., 2007).

In the first basic model of SOA formation using partitioning theory, Odum et al. (1996) used the measured yields of SOA obtained from smog chamber studies together with partitioning theory and was able to fit these yields by assuming that different amounts of two semi-volatile products were formed. This two-product model has been employed in a number of regional and global models (Chung and Seinfeld, 2002; Tsigaridis and Kanakidou, 2003; Liao et al., 2007; Carlton et al., 2010). These types of models can include the effect of changes in NO_x emissions on O_3 and the effects of NO_x on the abundance of reaction products by fitting to smog chamber results in high and low NO_x environments (Tsidigaris et al., 2006; Henze et al., 2008). They can also be extended to include more than two volatility products (Donahue et al., 2009).

However, this simple approach cannot account for the full complexity and the dynamics of SOA production. First, SVOC formation strongly depends on ambient conditions, e.g., temperature, photolysis, and most notably on the fate of RO_2, which can react with NO_x, HO_2, and other RO_2. This is usually described as a VOC: NO_x dependence. This dependence was parameterized in a simple way for aromatics by Henze et al. (2008) based on two different SOA product yields in low and high NO_x conditions (specifically, a high yield in low-NO_x conditions and a low yield in high NO_x conditions). But SOA formation is more complex and cannot be represented by these simple parameterizations. SOA formation from isoprene at high NO_x is also reduced (Kroll

et al., 2005a, 2006), while SOA formation is broadly similar at all NO_x levels in the ozonolysis of limonene (Zhang et al., 2006). Moreover, unlike aromatics and isoprene, SOA formation is increased at high NO_x in the photo-oxidation of sesquiterpenes (Ng et al., 2007). In addition, the SVOC products may be formed from first generation or higher generation products, and these products may undergo further reactions in the gas phase or aerosol phase (Ng et al., 2006; Camredon et al., 2007; Chan et al., 2007; Hallquist et al., 2009). As a consequence of these complexities and dynamics, the use of simple SOA yields from laboratory data may not account for the actual SOA system without a significant increase in the availability of these data and the complexity of the parameterizations.

In contrast to this empirical Odum-type model, a second type of model uses an explicit photochemical mechanism to form SVOC (e.g., Griffin et al., 2002; Zhang et al., 2004; Pun et al., 2006; Johnson et al., 2006; Camredon et al., 2007; Xia et al., 2008; Utembe et al., 2011), but may be limited in its ability to form SOA if the product distribution of SVOCs and their properties are incorrect. Nevertheless, we follow this philosophy here because this type of mechanism (1) is more explicit in its description of the oxidation products that lead to SOA formation, (2) handles the VOC:NO_x dependence in SVOC formation based on first principles as deduced in the explicit mechanism, (3) is easily extended as more knowledge of VOC oxidation schemes becomes available, and (4) predicts products that can be explicitly compared to observations.

In this explicit model, a detailed gas-phase mechanism is used to predict the formation of semi-volatile products, with gas-particle partitioning computed from an explicit calculation of K_i for each semi-volatile compound. To determine the semi-volatile compounds that might partition into the aerosol phase, we used the following criteria suggested by Griffin et al. (2002): (1) partially soluble; (2) an aromatic acid; (3) an aromatic compound with two functional groups that are not aldehydes; (4) 12 or more carbon atoms; (5) at least 10 carbon atoms and two functional groups; (6) at least six carbon atoms and two functional groups, one of which is an acid; and (7) tri-functional. From the above criteria, 26 species from the chemical mechanism described above that have the potential to produce SOA were selected (Table S1 in the Supplement). All the species were oxygenated derivatives from aromatics, isoprene, alpha-pinene, limonene and carbonyls.

The partitioning coefficient K_i for each compound listed in Table S1 in the Supplement is calculated explicitly according to:

$$K_i = \frac{RT}{10^6 \mathrm{MW} \zeta_i p^{\mathrm{o}}_{L,i}} , \quad (3)$$

where R (8.206×10^{-5} atm m^3 mol^{-1} K^{-1}) is the ideal gas constant, T (K) the temperature, MW (g mol^{-1}) the average molecular weight of the absorbing aerosol phase, ζ_i (dimensionless) the activity coefficient of the compound in the organic aerosol phase, $p^{\mathrm{o}}_{L,i}$ (atm) the compound vapor pressure (sub-cooled if necessary) and 10^6 is a unit conversion factor (g g^{-1}).

Since experimentally determined vapor pressures are not available for many species, we used the method of Myrdal and Yalkowsky (1997) to determine $p^{\mathrm{o}}_{L,i}$, with some changes added to include the particular chemical structure of the SOA forming compounds (Camredon and Aumont, 2006). The Myrdal and Yalkowsky method estimates the boiling point of a given organic compound based on the Joback group contribution method (Reid et al., 1987), and then estimates the vapor pressure at a given temperature. Similar methods have been used previously by Griffin et al. (2002), Zhang et al. (2004) and Pun et al. (2006). Camredon and Aumont (2006) showed that the Myrdal and Yalkowsky method provides good estimates of vapor pressure for a set of organic species of importance for SOA formation. There are, however, many methods in the literature that have been developed to estimate vapor pressure. Barley and McFiggans (2010) assessed the ability of different vapor pressure methods to predict vapor pressures of lower volatility compounds. As noted by Barley and McFiggans (2010), the Joback method for estimating boiling points tends to underestimate the amount of material that can partition to the aerosol phase. Nevertheless, Booth et al. (2010, 2011) used some new room temperature low vapor pressure data for polyfunctional compounds, especially acids and diacids, and showed that other methods (e.g., the method of Nannoolal et al., 2008) do not predict the data as well. Therefore, we should keep in mind uncertainties in the vapor-pressure estimates when drawing conclusions regarding the ability of this mechanism to reproduce observations. For example, Simpson et al. (2007) showed that the total modeled carbonaceous aerosol over Europe was very sensitive to the choice of vapor pressures. Valorso et al. (2011) tested the sensitivity of SOA formation from α-pinene photo-oxidation to three different vapor pressure estimation methods (i.e., Myrdal and Yalkowsky, 1997; Nannoolal et al., 2008, and the SIMPOL-1 method from Pankow and Asher, 2008), and found that the predicted SOA mass concentrations varied significantly from 8 to 28 μg m^{-3} in "high NO_x" experiments. Despite the sensitivity of SOA formation to different vapor pressure estimation methods, Camredon et al. (2010) found the best agreement with experimental aerosol yields of α-pinene dark ozonolysis experiments using the Myrdal and Yalkowsky method. Thus, we use this method here.

In the model represented by Eq. (3), the value of ζ_i is also uncertain. Several authors (e.g., Pankow, 1994 and Kamens et al., 1999) have assumed a value of one for oxidation products in an aerosol particle composed of a mixture of similar species. Although methods have been proposed to estimate the activity coefficient (Bowman and Karamalegos, 2002), we set ζ_i to one for simplicity.

The effect of temperature was taken into account according to the Clausius-Clapeyron equation using enthalpies of vaporization. However, the values for the enthalpy for most compounds are highly uncertain (Bilde and Pandis, 2001; Chung and Seinfeld, 2002; Donahue et al., 2006; Stanier et al., 2007; Saathoff et al., 2009; Epstein et al., 2010). In this paper, following other recent studies, we assume a value of 42 kJ mol^{-1} for all organic species for simplicity (Chung and Seinfeld, 2002; Liao et al., 2007; Heald et al., 2008). Table S1 shows the compounds that are allowed to partition to the aerosol phase, their parent VOC and the partitioning coefficients at a temperature of 298 K.

2.2.2 Formation of oligomers

Oligomer formation has been seen in both laboratory and atmospheric observations of SOA (Decesari et al., 2000; Gelencsér et al., 2002; Gross et al., 2006; Dommen et al., 2006; Iinuma et al., 2007). To incorporate this formation and other heterogeneous reactions that form low-volatility products in the aerosol phase into our model, we assumed that these compounds form with a time constant of 1 day following the reversible gas-particle partitioning process. This 1-day time scale is somewhat arbitrary, but is consistent with the Paulsen et al. (2006) laboratory study of oligomer formation. Support for the low-volatility of these products is provided by Vaden et al. (2011) who studied the evaporation kinetics of laboratory and ambient SOA and found that SOA evaporation is very slow (lasting more than a day), and by Perraud et al. (2012) who reported irreversible SOA formation from the oxidation of α-pinene by ozone and NO_3, which seems to contradict equilibrium gas-particle partitioning. Evidence for ambient low-volatility compounds was provided by Cappa and Jimenez (2010) who analyzed a thermodenuder dataset and concluded that a significant fraction of the atmospheric OA consisted of non-evaporative components. Since we do not have information on the volatility of these compounds, we make the expedient assumption that the oligomers which form do not evaporate. We note that the presence of oligomers within SOA would be expected to increase its MW, which typically ranges from 200–900 g mol^{-1} in laboratory observations (Gross et al., 2006; Sato et al., 2007; Dommen et al., 2006; Iinuma et al., 2007). This increase would be expected to decrease the partitioning coefficient, K_i. However, since we do not actually follow the chemical form of the oligomers in our model, we assumed that the molecular weight (MW) of the low-volatility products is equal to the MW of the absorbing semi-volatile compounds.

We note that the formation of oligomers in heterogeneous reactions within or on aerosols may be reversible or irreversible. Liggio et al. (2005a) had an experimental setup designed to look at kinetics and demonstrated that the reactions in the aerosol phase after uptake of glyoxal were irreversible on the 4 h time scale of their experiments. The experimental setup for Kroll et al. (2005b) was designed to look at equilibrium products. They examined the possible heterogeneous uptake and irreversible transformation of a number of simple carbonyl species (formaldehyde, octanal, trans-2, 4-hexadienal, glyoxal, methylglyoxal, 2,3-butanedione, 2,4-pentanedione, glutaraldehyde, and hydroxyacetone) onto inorganic seed aerosols. Only glyoxal was reported to substantially increase in the particle phase. Moreover, the lack of particle growth while gas phase glyoxal was still present in their system indicated that the uptake was fully reversible. These results are at odds with those of other researchers (Jang and Kamens, 2001; Jang et al., 2002, 2003a, b, 2005) who observed significant aerosol growth when inorganic seed was exposed to a wide variety of organic species. The compounds studied included simple C4–C10 aldehydes, unsaturated carbonyl compounds, and dicarbonyl compounds.

The rate of formation of oligomers used in our simple treatment is uncertain, and may vary with different compounds. While some laboratory studies showed that at least some of the oligomers are formed quite rapidly on a time scale of one minute (e.g., Heaton et al., 2007), several chamber studies of the chemical composition, volatility and hygroscopicity of SOA indicated that accretion reactions also take place on longer time scales (Gross et al., 2006; Paulsen et al., 2006; Dommen et al., 2006; Kalberer et al., 2006). Gross et al. (2006) demonstrated that high MW oligomeric species could be detected within 1 to 2 h (after turning the lights on) due to oligomerization reactions within the aerosol phase. Formation of these low volatility compounds continued for up to 20 h, with about 50–60 % of the SOA particle volume non-volatile at 100 °C for 1,3,5-trimethylbenzene after 5–6 h and 80 to 90 % of the SOA particle volume non-volatile for α-pinene generated SOA after 25 h (Paulsen et al., 2006). The rate of formation of oligomers in the Paulsen et al. (2006) study was of order 1 day for 1,3,5-trimethylbenzene and 3 days for a-pinene generated SOA, but might be slower in ambient aerosols, since the oligomer-forming compounds might be more dilute within ambient aerosol mixtures. The rate of formation of oligomers follows a chain growth polymerization model, wherein most of the molecular size develops rapidly followed by a continuous growth in the fraction of SOA that consists of oligomers (Kalberer et al., 2006). For isoprene in a low NO_x environment, the time constant for formation of low volatility products within the aerosol phase is about 2.3 days (Chan et al., 2007). In contrast to the Chan et al. (2007) study, Domen et al. (2006) observed that particles grew steadily within 8 h, mainly due to oligomers formed in the aerosol phase from isoprene photo-oxidation at high NO_x.

Smog chamber experiments have also shown that polymerization within the aerosol phase can be catalyzed by semi-volatile acidic reaction products (Kalberer et al., 2004). The smog-chamber study by Iinuma et al. (2005) examined the effect of acidic seed particles on α-pinene ozonolysis and suggested that acidity promotes SOA formation and

increases aerosol yields by up to 40 %. Surratt et al. (2007) examined SOA formation from isoprene and demonstrated that for low relative humidities (30 %), the range of acidities observed in atmospheric aerosols could increase SOA concentrations by a factor of two.

The above discussion demonstrates that oligomer formation seems ubiquitous, but the rate of formation may vary with compound and concentration. In addition, the possibility of reversible oligomerization should be considered as well, in light of the dependence of condensed phase reactions on the acidity of the existing aerosols. Nevertheless, our simple 1-day formation rate together with the assumption of irreversibility seems justified at this point in time, though we acknowledge the need to refine this part of model when additional experimental data become available. We note that oligomers contribute most of the SOA formed after gas-particle partitioning (see Table 4). We test the response of the model to an increase and a decrease in the time constant for formation in Sect. 5.

In summary, we use an explicit gas-phase mechanism to predict the formation of SVOCs, which can condense onto pre-existing aerosols through gas-particle partitioning. These condensed SVOCs are assumed to further react to form low-volatility compounds (i.e., oligomers) with a one-day time constant. Due to the lack of any detailed knowledge of their volatility, we assume that these compounds do not evaporate once they are formed. For convenience, we refer to these condensed SVOCs and their reaction products (oligomers), formed through the mechanism above, as sv_oSOA and ne_oSOA, respectively, (see Table 1). The abbreviation "sv" indicates "semi-volatile" and "ne" stands for "non-evaporative", since this is how the low-volatility compounds are treated in the model. "oSOA" stands for "other oxygenated SOA" to differentiate it from SOA formed from the uptake of glyoxal, methylglyoxal and epoxide, which is described in the next section.

2.2.3 Uptake of glyoxal, methylglyoxal and epoxide

In addition to examining the formation of SOA from the basic Ito et al. (2007) mechanism, we added the formation of SOA from glyoxal and methylglyoxal which form as a result of the oxidation of several VOCs. We also included the formation of SOA from epoxide formed in the oxidation of isoprene. Hereafter, we refer to these SOAs as ne_GLYX, ne_MGLY and ne_IEPOX, respectively (see Table 1). Over the past few years, glyoxal and methylglyoxal have gained great attention because of their potential importance to form SOA through aqueous phase reactions due to their high water solubility, their ability to form oligomers via acid catalysis, and their reactivity with OH radicals (Blando and Turpin, 2000; Volkamer et al., 2007; Carlton et al., 2007). Generally, these aqueous-phase reactions can be categorized as radical or non-radical reactions (Lim et al., 2010). Radical reactions can involve a variety of atmospheric oxidants – including OH radicals, NO_3 radicals, and O_3 – and can be initiated by photolysis. The chamber study of Volkamer et al. (2009) demonstrated that SOA formation through aqueous photooxidation of glyoxal was dramatic during daytime when the gas-phase OH radical concentration is about 10^7 molecules cm^{-3}. Non-radical reactions include hemiacetal formation (Liggio et al., 2005a; Loeffler et al., 2006), aldol condensation (Jang et al., 2002), imine formation (Galloway et al., 2009), anhydride formation (Gao et al., 2004), esterification via condensation reactions (Gao et al., 2004), and organosulfate formation (Liggio et al., 2005b; Surratt et al., 2007).

In this paper, we treat the SOA formation from glyoxal, methylglyoxal and epoxide, following the basic methods described by Fu et al. (2008, 2009) for glyoxal and methylglyoxal. Based on early laboratory evidence for irreversible surface-controlled uptake of glyoxal to aerosols (Liggio et al., 2005a, b), Fu et al. (2008, 2009) parameterized the loss of gas phase glyoxal and methylglyoxal on aqueous particles using the following equation:

$$\frac{dC_g}{dt} = \frac{1}{4} \cdot \gamma \cdot A \cdot < v > \cdot C_g \,, \quad (4)$$

where A is the total surface area of aqueous sulfate aerosols [m^2] and C_g is the concentration of gas phase glyoxal or methylglyoxal. The production of aqueous phase products can be directly equated to the loss of gas phase species. The parameter γ is the reactive uptake coefficient, representing the probability that a collision between a gas molecule and the aqueous particle surface will result in irreversible uptake considering processes such as diffusion, mass accommodation, dissolution and chemical reaction. The value of γ used in the Fu et al. (2008, 2009) studies was assumed 2.9×10^{-3} for both glyoxal and methylglyoxal, and we use the same value for epoxide here. In addition to treating uptake on aqueous particles, Fu et al. (2008, 2009) also included uptake by cloud droplets in a similar fashion, but accounting for diffusion limitation. Here, we also account for the uptake of glyoxal and methylglyoxal by cloud droplets in the same way as that in Fu et al. (2008, 2009).

It should be noted, however, that this simple treatment of irreversible surface-controlled uptake might be misleading if there is competition between reversible vs. irreversible uptake and bulk reactions vs. surface processes (Ervens and Volkamer, 2010). While aqueous photooxidation (e.g., aqueous-phase reactions of glyoxal with OH radical) of glyoxal can lead to products that are clearly formed through irreversible processes, Kroll et al. (2005b) and Galloway et al. (2009) report that glyoxal oligomers formed through acid catalyzed pathways are reversible. Furthermore, Ervens and Volkamer (2010) fit the observed glyoxal loss rates or observed SOA mass formation rates from different literature studies (i.e., Hastings et al., 2005; Liggio et al., 2005a; Volkamer et al., 2009) to a bulk-limitation equation expressing the SOA formation rate, and showed that the surface area of the aerosol population did not control the uptake

of glyoxal and its conversion to SOA mass. In spite of the high uncertainty associated with the processes leading to the formation of SOA from glyoxal and methylglyoxal, we use the compact and simplified representation adopted by Fu et al. (2008) to obtain a first order estimate of the significance of glyoxal and methylglyoxal uptake for secondary organic aerosol formation.

Paulot et al. (2009) demonstrated that isoprene photooxidation under low-NO_x conditions can generate high concentrations of gas-phase epoxydiols, which are observed to be a key gas-phase intermediate in the formation of SOA from isoprene at low-NO_x conditions (Surratt et al., 2010). The reaction kinetics for the formation of epoxydiols have recently been reported (Minerath et al., 2009a, b; Eddingsaas et al., 2010). These studies showed that acid-catalyzed ring-opening reactions of epoxides in the particle phase were kinetically favored under typical tropospheric conditions, leading to the formation of known isoprene SOA tracers (e.g., 2-methyltetrols and their corresponding organosulfates) (Claeys et al., 2004; Surratt et al., 2010). Also, these isoprene-derived epoxydiols and organosulfates were identified in ambient aerosols during several aircraft measurement campaigns (Froyd et al., 2010; Chan et al., 2010). Therefore, we added the uptake of epoxydiols by aqueous sulfate aerosols using the same formulation as that for glyoxal and methylglyoxal.

2.3 Emissions

Table 2 summarizes the global emissions of gas, aerosols and aerosol precursors used in the model. The emissions of gas-phase species are based on the paper by Ito et al. (2007, 2009) and the POA emissions on the paper by Wang et al. (2009), with some additions. We include both terrestrial and marine isoprene sources. Terrestrial isoprene emissions are based on a modified version of the inventory of Guenther et al. (1995) by Wang et al. (1998) and Bey et al. (2001), with a total biogenic isoprene source of 470.8 Tg C yr^{-1}. The total marine isoprene emission, with a value of 0.9 Tg C yr^{-1}, is from the estimate by Gantt et al. (2009) based on satellite observations. This total marine isoprene flux is scaled by monthly mean MODIS chlorophyll concentrations and surface wind speeds to determine the spatial and time variation of the flux (Palmer and Shaw, 2005). The biogenic terpene source is 117.6 Tg C yr^{-1} and is based on the work of Guenther et al. (1995) as modified by Wang et al. (1998). The other temperature-dependent BVOC emissions for ethane, propene, acetone, and methanol are distributed according to emissions of isoprene following Ito et al. (2007).

Sources of primary organic emissions in the model include organics from sea spray (35 Tg yr^{-1}), fossil fuel and biofuel emissions (16 Tg yr^{-1}), and open biomass burning (47 Tg yr^{-1}). The primary sea spray organic source was estimated using the correlation between chlorophyll *a* and the fractional water insoluble organic mass of sea salt, following O'Dowd et al. (2008), where the chlorophyll concentrations were those measured by MODIS Aqua averaged for the 5 yr from 2004 to 2008. The total marine organic aerosol is 35 Tg yr^{-1}, which is very close to the value given by Gantt et al. (2009) based on remote sensing (i.e., 22.3 Tg C yr^{-1} or 35.6 Tg yr^{-1} if the ratio of OM to OC is 1.6). Water soluble organic carbon (WSOC) is also present in marine aerosols

Table 2. Global emissions of gases, aerosols and aerosol precursors.

Species	Emission Rate
SO_2 or precursor	92.2 Tg S yr^{-1}
Fossil fuel and industry	61.3 Tg S yr^{-1}
Volcanoes	4.8 Tg S yr^{-1}
DMS	26.1 Tg S yr^{-1}
NO	42.1 Tg N yr^{-1}
Fossil Fuel	22.7 Tg N yr^{-1}
Biomass burning	9.3 Tg N yr^{-1}
Soil	5.5 Tg N yr^{-1}
Lighting	3.0 Tg N yr^{-1}
Aircraft	0.9 Tg N yr^{-1}
Ship	0.7 Tg N yr^{-1}
CO	426.0 Tg C yr^{-1}
MEK(>C3 ketones)	5.8 Tg C yr^{-1}
PRPE(>=C4 alkenes)	11.3 Tg C yr^{-1}
C_2H_6	9.3 Tg C yr^{-1}
C_3H_8	7.3 Tg C yr^{-1}
ALK4(>=C4 alkanes)	15.3 Tg C yr^{-1}
Acetaldehyde	3.3 Tg C yr^{-1}
CH_2O	2.4 Tg C yr^{-1}
ALK7(C6–C8 alkanes)	11.3 Tg C yr^{-1}
Benzene	3.2 Tg C yr^{-1}
Toluene	5.8 Tg C yr^{-1}
Xylene	3.9 Tg C yr^{-1}
trans-2-butene	6.6 Tg C yr^{-1}
HCOOH	2.6 Tg C yr^{-1}
acetic acid	12.4 Tg C yr^{-1}
Phenol	4.3 Tg C yr^{-1}
Ocean source of POA	34.5 Tg yr^{-1}
DMS source of MSA	8.2 Tg yr^{-1}
Fossil fuel + biofuel POA*	15.7 Tg OM yr^{-1}
Fossil fuel + biofuel BC	5.8 Tg BC yr^{-1}
Biomass burning OM*	47.4 Tg OM yr^{-1}
Biomass burning BC	4.7 Tg BC yr^{-1}
Isoprene	472.0 Tg C yr^{-1}
α-pinene	78.8 Tg C yr^{-1}
Limonene	38.8 Tg C yr^{-1}
PRPE(>=C4 alkenes)	24.2 Tg C yr^{-1}
Methanol	42.9 Tg C yr^{-1}
Acetone	44.5 Tg C yr^{-1}
Ethane	28.2 Tg C yr^{-1}

* Half of these POA emissions are assumed to be composed of low-volatility compounds that may have undergone reactions and partitioned back into the aerosol form as SOA.

and makes up 20–25 % of the total submicron mass (Yoon et al., 2007). It is likely produced through photochemical aging of volatile organic compounds, so has not been included in our primary marine source. We note that there is a large difference in the source strengths estimated from "bottom-up" and "top-down" methods (Gantt et al., 2009; Luo and Yu, 2010).

The concentration of the organic portion of the sea salt source was lumped together with the concentration of MSA produced from the oxidation of DMS within the code. For this source, we assumed a pathway based on the reaction of DMS with OH that produced only SO_2 (with a rate coefficient $9.6 \times 10^{-12} \exp\left(-\frac{234}{T}\right)$; and a pathway that forms 0.75 moles of SO_2 and 0.25 moles MSA, with a rate coefficient $\frac{k_1 M}{1+2k_2 M}$, where $k_1 = 1.7 \times 10^{-42} \exp\left(\frac{7810}{T}\right)$, $k_2 = 5.5 \times 10^{-31} \exp\left(\frac{7460}{T}\right)$ and $M = O_2$ (molecules cm^{-3}), following Gondwe et al. (2003) and references therein. The total annual average source of MSA is 8.23 Tg yr^{-1}.

Fossil fuel and biofuel emissions total 16 Tg yr^{-1}. These emissions were estimated by Ito and Penner (2005) for the year 2000, but Wang et al. (2009) adjusted the fossil fuel emissions to fit observed surface BC concentration and we use their adjusted emissions here. Open biomass burning emissions total 47.4 Tg yr^{-1}, and were developed based on using the Ito and Penner (2005) emissions for BC as an a priori estimate together with the inverse model approach of Zhang et al. (2005). The POM associated with open burning was then similarly scaled. While we have not considered primary emissions of semi-volatile organics or organics with intermediate volatility, we assume that half of our POA emissions are SOA. This assumption is simpler than the detailed modeling of semi-volatile emissions by Pye and Seinfeld (2010), but is generally consistent with their findings. The budget for these compounds follows that given in Table 3 for total POA, but the burden is only half the quantities shown there.

Table 3. Global budgets for organic aerosols from oceans and primary sources (Tg yr^{-1})*.

	This Work
POA from oceans	
Formation of MSA from DMS	8.2
Primary organics from sea spray	34.9
Dry deposition	5.1
Wet deposition	38.0
Burden	0.25
Lifetime (days)	2.1
Anthropogenic POA	
Fossil/bio fuel emission	15.7
Dry deposition	1.5
Wet deposition	14.2
Burden	0.13
Lifetime	3.0
Open burning emission	47.4
Dry deposition	3.7
Wet deposition	43.7
Burden	0.64
Lifetime	4.9

* Half of the anthropogenic POA emissions are assumed to be composed of low-volatility compounds that may have undergone reactions and partitioned back into the aerosol form as SOA.

2.4 Dry and wet deposition

We treat the dry deposition of gas phase species in the same manner as Ito et al. (2007), which uses the dry deposition algorithm described in Wang et al. (1998). Bessagnet et al. (2010) demonstrated the importance of dry deposition of semi-volatile organic compounds to the estimate of SOA concentrations. Karl et al. (2010) examined the effect of using different reactive factors f_0 for deposition. This factor accounts for the effect of the reactivity of different gases on the canopy resistance to mesophyll uptake (R_m), one of components contributing to the canopy surface resistance (R_c) (Wesely et al., 1989). They showed that using a value that was too small (i.e., $f_0 = 0$ or 0.1) for oxygenated VOCs underestimated their dry deposition removal rate compared to ecosystem-scale flux measurements. In this paper, we use the same dry deposition loss rate for SVOCs as that for PAN, i.e., a reactive factor f_0 of 0.1. Gravitational settling is taken into account for aerosol species. The settling velocity and the slip correction factor for Stokes law are calculated from Seinfeld and Pandis (1998) using the mass-weighted average radius in each size bin for each aerosol component, based on the assumed dry size distribution and its growth with relative humidity. Wet deposition is calculated using the scavenging module developed by Mari et al. (2000) and Liu et al. (2001), which includes scavenging in convective updrafts and first-order rainout and washout in precipitating columns. The horizontal fractional area of each grid box experiencing precipitation is based on the work by Giorgi and Chameides (1986), assuming a cloud liquid water content of 1.5 g m^{-3} for stratiform cloud and 2.0 g m^{-3} for convective cloud. Wet removal of gas-phase organic compounds is calculated based on the Henry's law constant. We adopted Henry's law coefficients for gas-phase species from Ito et al. (2007). The scavenging efficiencies of OA as well as other aerosol types are equal to the mass fraction of OA that is activated to cloud droplets in liquid clouds. The calculation of the mass fraction is based on the cloud droplet activation parameterization of Abdul-Razzak and Ghan (2000, 2002). The detailed description of the cloud activation parameterization may be found in Wang and Penner (2009).

Table 4. The global burden, production and lifetime for each SOA component.

		sv_oSOA	ne_oSOA	ne_GLYX	ne_MGLY	ne_IEPOX	Total SOA
Burden (Tg)	Simulation A	0.06	0.54	0.15	0.34	0.56	1.65
	Simulation B	0.04	0.39	0.19	0.26	0.20	1.08
	Simulation C	0.07	0.62	0.20	0.30	0.35	1.54
Total production ($Tg\,yr^{-1}$)	Simulation A	7.0	24.5	13.5	38.3	37.2	120.5
	Simulation B	5.8	17.8	22.2	32.1	12.9	90.8
	Simulation C	8.1	26.6	22.6	36.9	25.1	119.3
Anthropogenic production ($Tg\,yr^{-1}$)	Simulation A	1.1	3.7	2.5	5.9	0.0	13.2
	Simulation B	1.1	3.4	2.7	6.6	0.0	13.8
	Simulation C	1.1	3.6	2.6	6.4	0.0	13.7
Biogenic production ($Tg\,yr^{-1}$)	Simulation A	5.9	20.8	11.0	32.4	37.2	107.3
	Simulation B	4.7	14.4	19.5	25.6	12.9	77.0
	Simulation C	7.0	23.0	20.0	30.5	25.1	105.6
Lifetime (days)	Simulation A	3.1	8.1	4.1	3.2	5.5	5.0
	Simulation B	2.5	8.0	3.1	3.0	5.7	4.3
	Simulation C	3.1	8.5	3.2	3.0	5.1	4.7

3 Results

Here we summarize our model predictions for SOA and OM and compare these to measurements. Liu et al. (2005) provided a thorough evaluation of the model-predicted sulfate, black carbon, dust, and sea salt so this is not repeated here.

3.1 Budget calculation

The budget of POA from ocean sources and fossil fuel and biomass burning is shown in Table 3. The atmospheric burden of organics from the oceans is 0.25 Tg, with a lifetime of 2.1 days. This lifetime is somewhat shorter than the lifetime for the average over all organics in the standard version of the IMPACT model (Liu et al., 2005), which is 3.2 days, and may reflect the fact that most of the current source only injects POA into the lowest model layer over the oceans. The total atmospheric burden of fossil and biofuel POA is 0.13 Tg, while for biomass burning it is 0.64 Tg. The lifetime for the surface-based fossil and biofuel emissions is 3.0 days, while for open burning it is 4.9 days. The average lifetimes computed here differ somewhat from that in Liu et al. (2005) because our scavenging treatment has been adjusted to reflect the mass fraction of OM that acts to form cloud droplets as a cloud condensation nuclei.

Table 4 summarizes the production and the burden for the three simulations performed in this study (i.e., Simulation A without HO_x recycling, Simulation B with Peeters et al. (2009) HO_x regeneration, and Simulation C with reduced HO_x recycling rate). The total production rate of SOA in Simulation A is $120\,Tg\,yr^{-1}$. A little more than 62 % of the production rate is approximately evenly split between sources associated with methylglyoxal and epoxide, while 26 % is associated with sv_oSOA and ne_oSOA and 11 % with glyoxal. The introduction of the HO_x recycling mechanism of Peeters et al. (2009) has a large impact on the global average SOA burden and production rate. Both the total burden and production rate decrease by about 30 % in comparison to that of Simulation A, whereas the burden in Simulation C is only 5 % smaller than that in Simulation A. This reduction is caused by the competition of the 1, 5- and 1, 6-H shift reactions of the isoprene peroxy radicals with their traditional bimolecular reactions (e.g., reactions with NO and HO_2), which reduces the epoxide formation rate more than it is increased due to the increase in OH and HO_2. A detailed analysis of this competition will be described below. The burden and source strength in Simulation C lies between those in Simulation A and Simulation B.

The global budget of SOA is very uncertain. Recent top-down estimates based either on the mass balance of VOCs or on scaling to the sulfate budget suggest a global source strength ranging from 140–$910\,Tg\,C\,yr^{-1}$ (Goldstein and Galbally, 2007; Hallquist et al., 2009), corresponding to 280–$1820\,Tg\,yr^{-1}$ if the ratio of total OA to OC is 2.0 (Tupin and Lim, 2001). A more recent top-down estimate of the total OA budget using satellite observations of aerosol optical depth and a global model (Heald et al., 2010) was consistent with an SOA source of $150 \pm 120\,Tg\,C\,yr^{-1}$, corresponding to $300 \pm 240\,Tg\,yr^{-1}$ if one assumes an OA:OC ratio of 2:1. In addition, Spracklen et al. (2011) estimate a SOA source ranging from 50 to $230\,Tg\,yr^{-1}$, based on fitting the results of a global chemical transport model to aerosol mass spectrometer (AMS) observations. In contrast to these top-down estimates, traditional bottom-up estimates from global models that use known or inferred biogenic and/or anthropogenic VOC precursor fluxes together with laboratory data

Table 5. Global modeling studies of SOA precursor emissions, SOA production, burden and lifetime (Eb: emissions of biogenic species (i.e., isoprene and monoterpenes); Ea: emissions of anthropogenic species (i.e., aromatics); Pb: SOA production from biogenic species; Pa: SOA production from anthropogenic species; Pt and Bt: total SOA production and SOA burden).

References	Global Model	SOA model	Eb ($Tg\,yr^{-1}$)	Ea ($Tg\,yr^{-1}$)	Pb ($Tg\,yr^{-1}$)	Pa ($Tg\,yr^{-1}$)	Pt ($Tg\,yr^{-1}$)	Bt (Tg)	Lifetime (day)
O'Donnell et al. (2011)	ECHAM5-HAM	2-product	537	17	21.0	5.6	26.6	0.83	11.4
Heald et al. (2008)	CAM3	2-product	539[a]	16[a]	22.9[a]	1.4[a]	24.3[a]	0.59[a]	8.9
Farina et al. (2010)	GISS II	volatility basis	736	49	27.28	1.62–11.02[b]	28.9–38.3[b]	0.54–0.98[b]	6.8–9.4[b]
Utembe et al. (2011)	STOCHEM	explicit chemistry	628	60	21.1	1.4	22.5	0.23	3.7
Hoyle et al. (2009)	Oslo CTM3	2-product	386[a]	21.6[a]	–	–	53.4–68.8[c]	0.50–0.7[c]	3.4–3.7[c]
Tsigaridis and Kanakidou (2007)	TM3	2-product	747.2	15.8	16.8	1.8	18.6	0.82	16.0
Henze et al. (2008)	GEOS-Chem	2-product	635.2	18.8	26.8	3.5	30.3	0.81	9.8
Fu et al. (2008)	GEOS-Chem	2-product[d]	570	9.8	26.7[a]	2.3[a]	29[a]	0.62[a]	7.8
This work	IMPACT	explicit chemistry	589.6[a]	12.9[a]	77.0–107.3	13.3–13.8	90.8–120.5	1.08–1.65	4.3–5.0

[a] reported in Tg carbon and converted here using a 2:1 ratio of OM:OC, [b] high estimate assumes chemical aging of anthropogenic SOA, [c] high estimate assumes partitioning with sulfate, [d] includes irreversible uptake of glyoxal and methlyglyoxal

from oxidation experiments give much lower SOA production rates of 14–82 $Tg\,yr^{-1}$ (Hallquist et al., 2009).

When comparing with some other global chemical transport model bottom-up estimates (Table 5), our SOA production rates are larger in all simulations, but are well within the range deduced by Heald et al. (2010) and Spracklen et al. (2011). This higher source of SOA formation mainly comes from the irreversible uptake of gas phase glyoxal, methylglyoxal and IEPOX, which are not taken into account in traditional two-product models. Actually, our source of sv_oSOA and ne_oSOA, as indicated in Table 4, is comparable to the SOA sources reported for other models. Table 5 also breaks down the sources into those from anthropogenic emissions and those from biogenic emissions. The dominance of biogenic SOA production also agrees well with previous global model results. The fraction of biogenic production in our simulations, 84.8–89.0 %, is similar to that from previous models, i.e., typically 80–95 %. The lifetime of total SOA in the model (4–5 days) is somewhat shorter than that from other models, except for the results reported by Utembe et al. (2011). This shorter lifetime is mainly due to the larger removal rate coefficients from wet scavenging. One reason for the larger wet removal rates in our model is that most carbonaceous aerosols are internally mixed with sulfate and are generally hygroscopic, except very close to source regions (Liu et al., 2005).

The oligomer formation rates for SVOCs that partition to the aerosol phase are summarized in Table S1, as well as the relative contribution (annual mean) of various biogenic and anthropogenic species to the total ne_oSOA. Among these precursors, PRN2, or isoprene-hydroxy-nitrate, makes the greatest contribution to total ne_oSOA (54 %, 45 % and 39 % in Simulation A, B, and C, respectively). The global average source of PRN2 is mainly from the reaction of RIO_2 (RO_2 from isoprene) with NO, although it also comes from some other reactions (e.g., the reaction of RO_2 from monoterpenes with NO). The reaction of RIO_2 with NO competes with the isomerization through the 1,5-H shift or 1,6-H shift. This competition reduces the PRN2 formation rate from the reaction of RIO_2 with NO. As a result, the PRN2 SOA production rate is decreased to 8.1 $Tg\,yr^{-1}$ in Simulation B from 13.4 $Tg\,yr^{-1}$ in Simulation A. Not surprisingly, the PRN2 production rate in Simulation C is higher than that in Simulation B.

The total anthropogenic source of sv_oSOA and ne_oSOA in Simulation A is 4.8 $Tg\,yr^{-1}$, while that from biogenics is 26.7 $Tg\,yr^{-1}$ (Table 4). The lifetime of ne_oSOA is 8.1 days. This lifetime is much longer than that of the other SOA components. One reason for this longer lifetime is the longer lifetimes of the precursors, which make them more likely to be transported to higher altitudes prior to the formation of SOA, where dry and wet deposition are less efficient. The lifetime of gas-phase PRN2, which contributes the most to ne_oSOA, is about 9 h, which is longer than that of glyoxal and methylglyoxal (see Table 6). Another reason for the longer lifetime of ne_oSOA can be related to the temperature dependence of the gas-aerosol partition coefficients (Tsigaridis and Kanakidou, 2003; Hoyle et al., 2007). The lower temperature in the upper atmosphere favors condensation to form sv_oSOA on pre-existing aerosols, thereby also forming more ne_oSOA.

Table 6 shows the budget for the glyoxal, methylglyoxal, and epoxide SOA precursors. For Simulation A, the model predicts a total methylglyoxal formation rate of 156 $Tg\,yr^{-1}$ from biogenic sources, with 26 $Tg\,yr^{-1}$ from anthropogenic sources and 2.2 $Tg\,yr^{-1}$ from acetone (which is a mixture of anthropogenic and biogenic sources). These may be compared to the source strengths reported by Fu et al. (2008) of 116 $Tg\,yr^{-1}$, 16 $Tg\,yr^{-1}$ and 10 $Tg\,yr^{-1}$, respectively. Loss is primarily through photolysis (97 $Tg\,yr^{-1}$) and reaction with OH (43 $Tg\,yr^{-1}$), followed by the uptake by cloud drops (30 $Tg\,yr^{-1}$) and sulfate aerosols (8 $Tg\,yr^{-1}$). Our reaction with OH and on sulfate aerosols and clouds is a somewhat larger proportion of the total loss rate than that in Fu et al. (2008), and photolysis is somewhat less efficient than in Fu et al. (2008). If we add the HO_x recycling mechanism for isoprene oxidation, we produce less methylglyoxal

Table 6. Budgets for secondary organic aerosol precursors reacting on acidic aerosols and cloud drops ($Tg\,yr^{-1}$).

Glyoxal				
	Simulation A	Simulation B	Simulation C	Other work
Total sources	48.97	65.72	70.12	95–105 (Stavrakou et al., 2009)
Biogenic sources	39.95	57.78	62.16	24.28 (Fu et al., 2008)
Anthropogenic sources	9.02	7.94	7.96	20.47 (Fu et al., 2008)
Sinks				
Reaction with OH	10.0	15.3	14.8	6.5 (Fu et al., 2008)
Reaction with NO_3	0.02	0.03	0.03	< 0.1 (Fu et al., 2008)
Photolysis	23	23	28	28 (Fu et al., 2008)
Aerosol formation on cloud drops	10.4	16.9	17.8	5.5 (Fu et al., 2008)
Aerosol formation on sulfate aerosols	3.19	5.32	4.82	0.94 (Fu et al., 2008)
Wet deposition	1.6	3.2	3.1	1.9 (Fu et al., 2008)
Dry deposition	0.9	2.1	1.9	2.2 (Fu et al., 2008)
Burden	0.0170	0.020	0.022	0.015 (Fu et al., 2008)
Lifetime (hours)	3.0	2.7	2.8	2.9 (Fu et al., 2008)
Methylglyoxal				
	Simulation A	Simulation B	Simulation C	Fu et al. (2008)
Total sources	184.5	143.2	167.6	131.8
Biogenic sources	156.3	114.3	138.7	115.6
Anthropogenic sources	26.0	25.6	25.9	16.2
Acetone	2	3	3	10
Sinks				
Reaction with OH	43	44	46	15
Reaction with NO_3	9.6×10^{-2}	7.0×10^{-2}	8.3×10^{-2}	< 0.1
Photolysis	97	63	80	100
Aerosol formation on cloud drops	30	25	29	14
Aerosol formation on sulfate aerosols	7.9	7.5	7.8	1.4
Wet deposition	3.1	2.8	3.2	1.8
Dry deposition	1.8	1.9	2.0	1.7
Burden	0.037	0.027	0.032	0.025
Lifetime (hours)	1.8	1.7	1.7	1.6
Epoxides from isoprene				
	Simulation A	Simulation B	Simulation C	
Formation of IEPOX	195.2	78.5	150.7	
Sinks				
reaction with OH	157.9	65.8	125.5	
Converted to SOA	37.2	12.9	25.1	
Burden	0.259	0.063	0.145	
Lifetime (hours)	11.6	7.0	8.4	

(Simulation B), which is close to that reported by Fu et al. (2008). More methylglyoxal is again predicted in Simulation C when the rates of the 1,5-H and 1,6-H shifts in isoprene peroxy radicals are reduced.

The inclusion of the Peeters et al. (2009) HO_x recycling mechanism in Simulation B increases the rate of production of glyoxal by about 34 % compared to that in simulation A, while decreasing the rates of the 1,5-H and 1,6-H shift increases the glyoxal production rate by about 6 %. The total source of glyoxal from Simulation A is $49\,Tg\,yr^{-1}$. This is similar to the total source in Fu et al. (2008), but the proportion of our source from biogenics (89 %) is much higher than that in Fu et al. (2008) (i.e., 54 %). This source is significantly smaller, however, than the estimate of Stavrakou et al. (2009), $95–105\,Tg\,yr^{-1}$, which was based on inverse modeling to fit satellite observations of glyoxal. Because our lifetime of glyoxal is similar to that of Stavrakou et al. (2009) (i.e., 3.0 h vs. 2.5 h), we conclude that our glyoxal production rate may be too low to reproduce the satellite observations. The production rate of glyoxal is also relatively

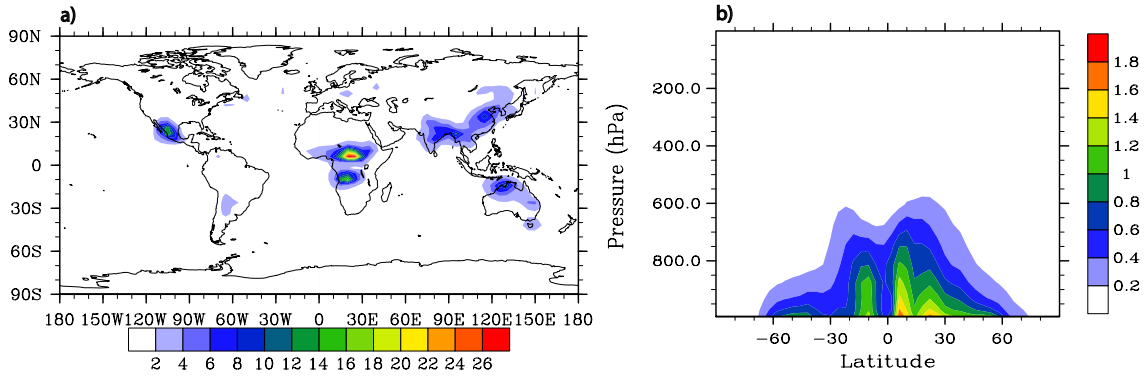

Fig. 1. Annual mean simulated surface POA concentrations **(a)** and zonal distrutubion of POA concentrations **(b)**. Units: $\mu g\,m^{-3}$.

low in the other two simulations. The proportion of our sink from the reaction of glyoxal with OH and from the formation of aerosols is higher than that by Fu et al. (2008) in all three simulations.

The only pathway to produce epoxides is reaction of RIO with HO_2. The introduction of the Peeters et al. (2009) HO_x recycling pathway decreases the production of epoxides in spite of the increase in RIO_2 and HO_2 concentrations. Most of the epoxides are lost by reaction with OH, and about 20 % reacts on sulfate aerosol to form organic aerosols.

The above secondary organic source gases result in total secondary organic aerosol burdens of 0.15, 0.34, and 0.56 Tg for ne_GLY, ne_MGLY and ne_IEPOX, respectively, in Simulation A. The lifetimes of these components are 4.1, 3.2 and 5.5 days. The inclusion of the Peeters et al. (2009) HO_x recycling mechanism makes the lifetime of ne_GLYX and ne_MGLY slightly shorter while slightly increasing the lifetime of ne_IEPOX. The reason for the shorter aerosol lifetime is related to the shorter lifetimes of the corresponding gas-phase precursors (Table 6). Higher OH concentrations in Simulation B consume glyoxal and methylglyoxal more efficiently so that they have shorter lifetimes. For ne_IEPOX, although its precursor epoxide also has a shorter lifetime when the HO_x recycling mechanism is included, the geographical distribution has changed (Fig. 2), with its peak concentration shifting from tropical regions with frequent precipitation to North America and East Asia with less precipitation. This change causes a smaller wet deposition flux of ne_IEPOX.

3.2 Global and vertical distributions

Figures 1 and 2 show the annual mean simulated concentrations of POA and SOA at the surface, respectively. The surface distribution of POA shows high concentrations in areas where significant biomass burning occurs. This pattern is consistent with the global average source from biomass burning, which contributes 75.1 % of the global average primary organic aerosols from combustion sources. The geographical distribution of SOA also reflects precursor emissions, with large concentrations of biogenic (isoprene) SOA in the tropics and in the southeastern United States. The SOA from gas to particle partitioning (sv_oSOA and ne_oSOA) shows a surface peak over Africa, which tracks POA to a certain extent. This correspondence between POA and sv_oSOA is related to the fact that the formation of sv_oSOA depends on both the supply of SOA precursors and oxidants and the presence of POA as a partitioning medium. On the other hand, the formation of ne_MGLY, ne_GLYX and ne_IEPOX are related to the sulfate concentration to some extent, which is reflected in the strong peaks in their surface concentrations near polluted areas in the Northern Hemisphere.

The change of each SOA component and total SOA between Simulation A and Simulations B and C is also shown in Fig. 2. Generally, the introduction of the Peeters et al. (2009) isoprene mechanism decreases sv_oSOA, ne_oSOA and ne_IEPOX surface concentrations and increases ne_GLYX surface concentrations, which is consistent with the change in global sources as described above. ne_MGLY surface concentrations change very little between Simulation A and Simulations B and C. Most regions show a decrease in the total SOA between Simulation B and A, consistent with the decreases in sv_oSOA, ne_oSOA and ne_IEPOX. Slowing the rates of the 1,5-H and 1,6-H shifts in isoprene radicals in Simulation C causes all the surface SOA component surface concentrations to increase compared to Simulation B, and the total SOA at the surface is larger than in Simulation A.

The zonal average vertical distribution of POA and SOA is shown in Figs. 1b and 3. The high concentrations of POA and SOA in the tropics near the surface (below 700 hPa) are consistent with the biomass burning sources and the significant SOA formation from biogenic precursors, respectively, as described above. One obvious feature of the ne_oSOA plot is that there is sustained SOA production in the free troposphere due to the relatively long lifetimes of ne_oSOA precursors and the colder temperatures in the free troposphere compared to those at the surface, causing a maximum in its concentration near 750 hPa.

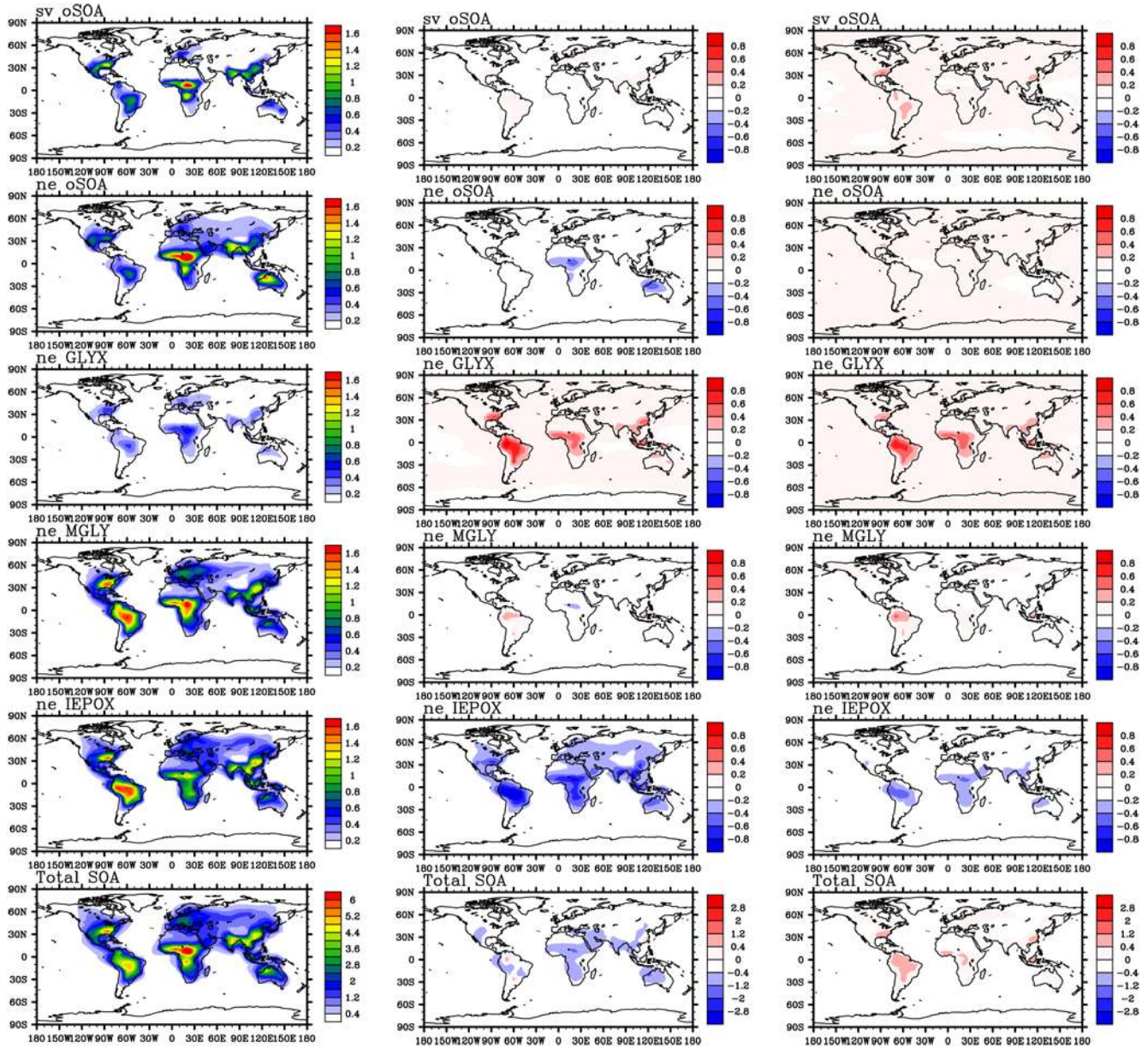

Fig. 2. Annual mean simulated surface SOA concentrations in Simulation A (first column) and the changes in surface SOA concentrations from Simulation A after including the new HO_x recycling mechanism (Simulation B-Simulation A) in the second column, and reducing the reaction rates of 1,5-H and 1,6-H shifts by a factor 10 (Simulation C-Simulation A) in the third column for each SOA component (the first 5 rows) and the total SOA (the sixth row). The maximum and minimum values for color scales in the second and third column are set to half the maximum values of those in the first column (Simulation A). Units: $\mu g\,m^{-3}$.

4 Comparison with measurements

4.1 Surface measurements

Figure 4a shows a comparison of annual mean model predicted and measured OA concentrations (from March 1996 to February 1999) in the United States for the 48 sites of the Interagency Monitoring of Protected Visual Environments (IMPROVE) network (Malm et al., 2000). Measurement data are reported as organic carbon (OC) in micrograms of carbon per cubic meter, while the model predicts organic mass (OM) concentrations. To convert OM to OC, we use a factor of 1.4 for POA and 1.8 for ne_oSOA. These factors are based on Tupin and Lim (2001) who suggested an average of 1.6 ± 0.2 for OM:OC ratio for urban OA and 2.1 ± 0.2 for more-oxygenated background aerosol. For other SOA components, we converted OM to OC based on their molecular mass and carbon number (i.e., 2.4 for

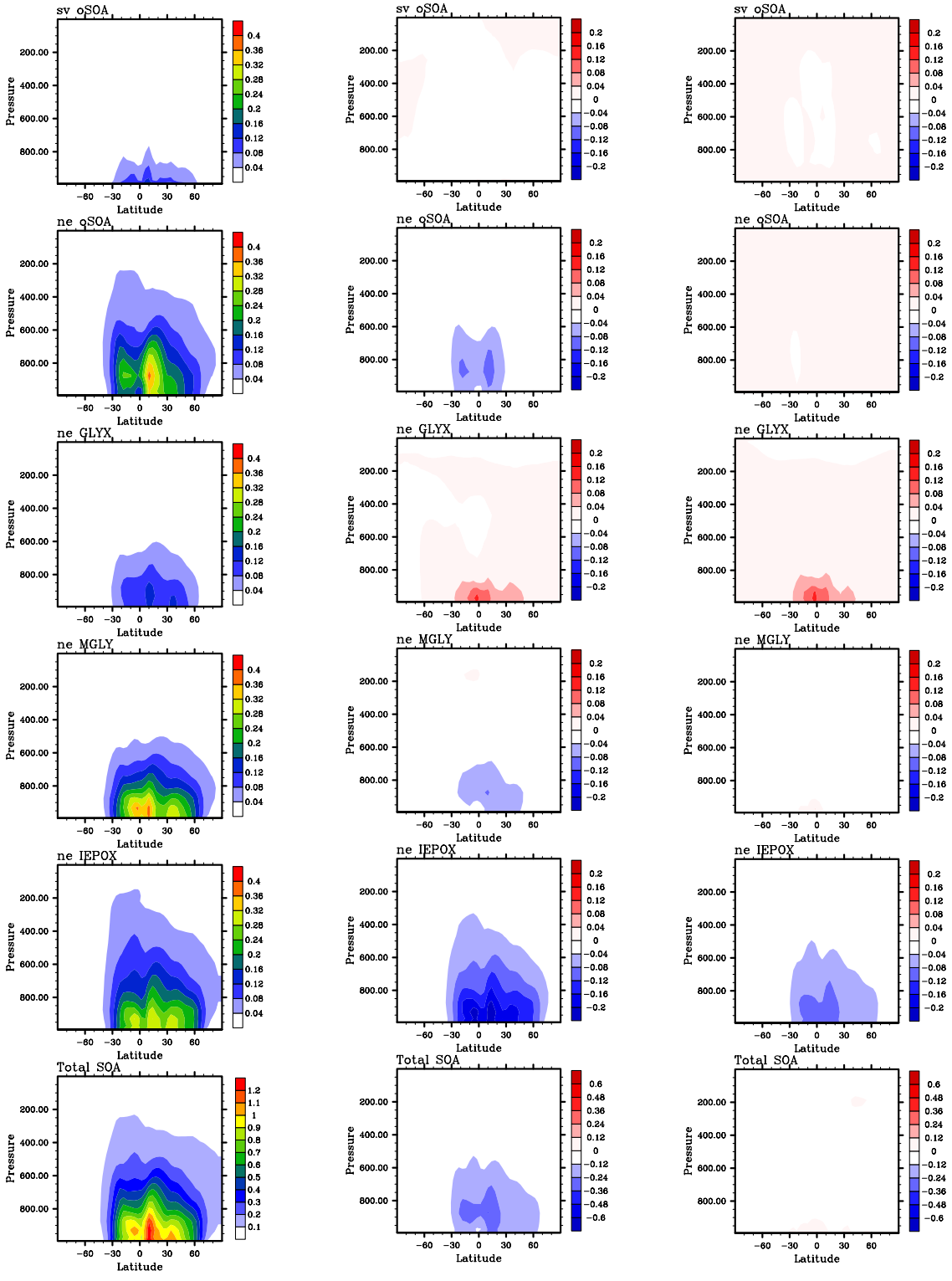

Fig. 3. Annual zonal mean simulated SOA concentrations in Simulation A (first column) and the changes in vertical distributions of SOA concentrations from Simulation A after including the new HO_x recycling mechanism (Simulation B–Simulation A) in the second column, and reducing the reaction rates of 1,5-H and 1,6-H shifts by a factor 10 (Simulation C–Simulation A) in the third column for each SOA component (the first 5 rows) and the total SOA (the sixth row). The maximum and minimum values for color scales in the second and third column are set to half the maximum values of those in the first column (Simulation A). Units: $\mu g\, m^{-3}$.

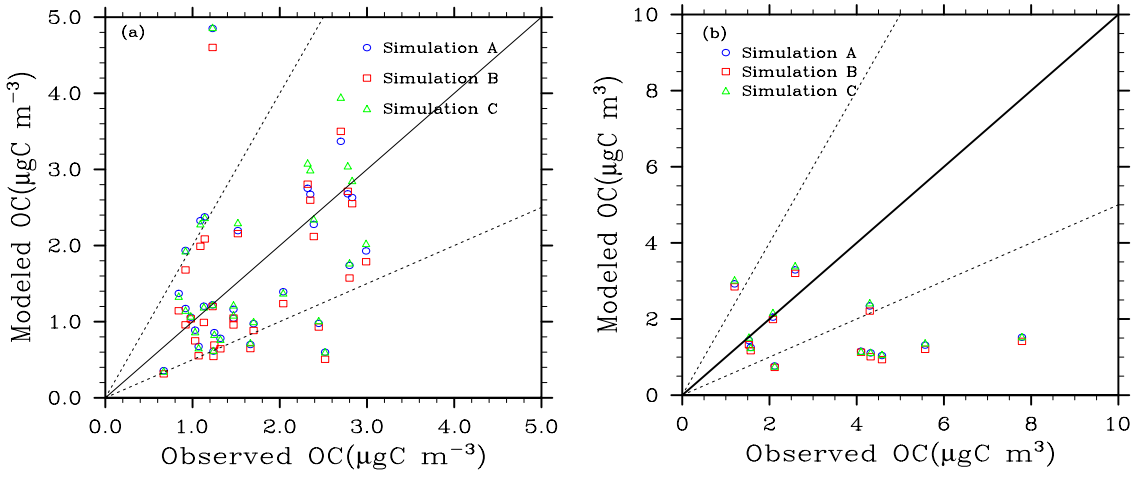

Fig. 4. Total annual averaged organic aerosol model comparison with the IMPROVE **(a)** and EMEP **(b)** observation networks. The solid lines represent ideal agreement (1:1 ratio), and the dashed lines are the 2:1 and 1:2 ratios, i.e., indicating agreement within a factor of 2. The IMPROVE network data are from 1996 to 1999, and the EMEP measurements were made in 2002–2003. The meteorology data used to run the model were for 1997.

Table 7. Normalized mean bias (NMB) and correlation coefficient (R) between the predicted SOA for the simulation and observations. The number of sites in the comparison is in parentheses.

Simulation name	AMS measurements (Zhang et al., 2007)					
	Urban sites ($N = 14$)		Urban downwind sites ($N = 6$)		Rural sites ($N = 17$)	
	NMB	R	NMB	R	NMB	R
Simulation A	−15.2 %	0.75	5.8 %	0.85	15.7 %	0.33
Simulation B	−23.0 %	0.74	−8.9 %	0.86	6.5 %	0.34
Simulation C	−12.5 %	0.72	8.9 %	0.86	20.0 %	0.30
	IMPROVE network ($N = 48$)					
	Annual average		Summer		Winter	
	NMB	R	NMB	R	NMB	R
Simulation A	−2.4 %	0.35	10.1 %	0.37	−15.0 %	0.38
Simulation B	−9.3 %	0.39	−4.8 %	0.44	−14.2 %	0.40
Simulation C	1.7 %	0.41	16.8 %	0.44	−13.8 %	0.40

ne_GLYX, 2.0 for ne_MGLY and 1.9 for ne_IEPOX). As shown in Fig. 4a, the simulated concentrations for most of the IMPROVE sites are generally within a factor of 2 of the observed concentrations. The annual mean OA concentrations have a mean bias (MB) of $-0.04\,\mu g\,C\,m^{-3}$ and a normalized mean bias (NMB) of −2.4 % for Simulation A, a MB of $-0.16\,\mu g\,C\,m^{-3}$ and NMB of −9.3 % for Simulation B, and a MB of $0.03\,\mu g\,C\,m^{-3}$ and NMB of 1.7 % for Simulation C (Table 7). The correlation coefficients (R) between observations and simulations for these three simulations are around 0.40 (Table 7), which indicates that the model does not capture the observed spatial variability well in North America. Figure 5 shows the simulated versus measured seasonal mean OA concentrations for the IMPROVE sites in summer and winter and the values of NMB and R for these comparisons are shown in Table 7. While the model slightly over-estimates the observations in the summer, the comparison in the winter has a NMB of around −15 %. The correlation coefficients for the summer and winter are similar to that in the annual mean comparison.

Chung and Seinfeld (2002) compared their results with observations from the IMPROVE network and reported that OM concentrations were consistently under-predicted by a factor of 3 or more. Park et al. (2003) showed a small bias (∼20 %) in predicted OC concentrations when compared to IMPROVE sites for the year 1998. Liao et

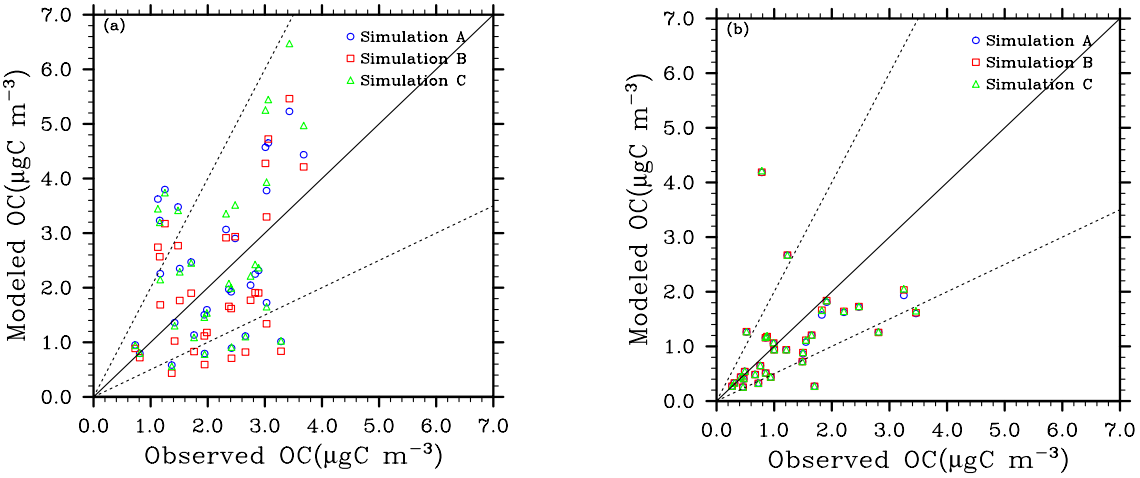

Fig. 5. Simulated versus observed seasonal mean OC concentrations for the IMPROVE network. **(a)** summer (JJA) and **(b)** winter (DJF). The solid lines represent ideal agreement (1:1 ratio), and the dashed lines are the 2:1 and 1:2 ratios. The IMPROVE network data are from 1996 to 1999. The meteorology data used to run the model were for 1997.

al. (2007) under-predicted OM relative to measurements over the United States with a NMB of −34.2 %. Farina et al. (2010) found that their model under-predicted OM by ∼26 % when compared to the IMPROVE network. This model included the chemical aging of anthropogenic SOA by gas-phase reaction of the SOA component with the hydroxyl radical. Both Park et al. (2003) and Farina et al. (2010) reported spatial pattern correlation coefficients R of around 0.65. Liao et al. (2007) compared the observed seasonal mean surface OA concentrations in the IMPROVE network and obtained correlation coefficients (R) in different seasons that ranged from 0.4 to 0.7.

Figure 4b compares the model results to measurements taken in Europe during a one-year campaign performed in 2002–2003 that focused on elemental and organic carbon as part of the European Monitoring and Evaluation Program (EMEP) (Yttri et al., 2007). Again, we used a scaling factor of 1.4 for POA and 1.8 for ne_oSOA to convert from units of OM to units of OC. In contrast to the comparison with the IMPROVE stations, the results of the model are significantly lower than all of the corresponding observations. The average concentrations observed at EMEP sites, however, are much higher than in the IMPROVE dataset, as PM_{10} measurements were reported at the EMEP sites vs. $PM_{2.5}$ in the IMPROVE network. These large particles are not captured in the model because we assume that all organics are only present as submicron particles. To gain further insight into the reasons for the difference between the model and observations, we examined the results for the summer and winter, respectively (Fig. 6). From the figure, it can be seen that SOA dominates OM in the summer and POA dominates in the winter when POA sources are larger (e.g., biomass burning) and isoprene emissions are low, consistent with other studies (Szidat et al., 2006; Simpson et al., 2007). Gelencsér et al. (2007) analyzed the $PM_{2.5}$ organic aerosol over Europe from the CARBOSOL project and concluded that biomass burning primary emissions were a significant contributor to OC in winter. Therefore, a possible reason for the wintertime discrepancy is that the emissions from domestic wood combustion are not fully represented in our emission database. To examine this hypothesis, we compared the model results with the corresponding components from the source-apportionment analysis of CARBOSOL in Gelencsér et al. (2007) for two surface sites (Aveiro, K-Puszta) (Table 8), as did Simpson et al. (2007). It may be of interest to also include the other two mountain sites, but surface sites reflect the boundary layer sources of OA (e.g., biomass burning) more directly. In addition, the comparisons with these surface sites are more comparable to evaluations that use the EMEP network for which most observations are near the surface. Recently, Gilardoni et al. (2011b) specifically distinguished primary and secondary biomass burning organic carbon from primary and secondary fossil organic carbon as well as biogenic organic carbon by using a combined ^{14}C – macro tracer analysis in Ispra, a site in northern Italy. Here we also compare our model results with their analysis in Table 8. Obviously, the primary biomass burning organic carbon is significantly underrepresented in the model. This may be due to the coarse resolution of the model, which cannot resolve the effects of local emissions. Another possible reason for the wintertime discrepancy is that the emissions from domestic wood combustion are too low in our emission database, which was also found in other model comparisons in Alpine Valleys (Szidat et al., 2007) and Ispra (Gilardoni et al., 2011b) during winter. For SOA, the model generally underestimates the observations. The SOA at the other European sites, therefore, is likely also underestimated in the model. The underestimation of SOA in Europe may be caused by the underestimation

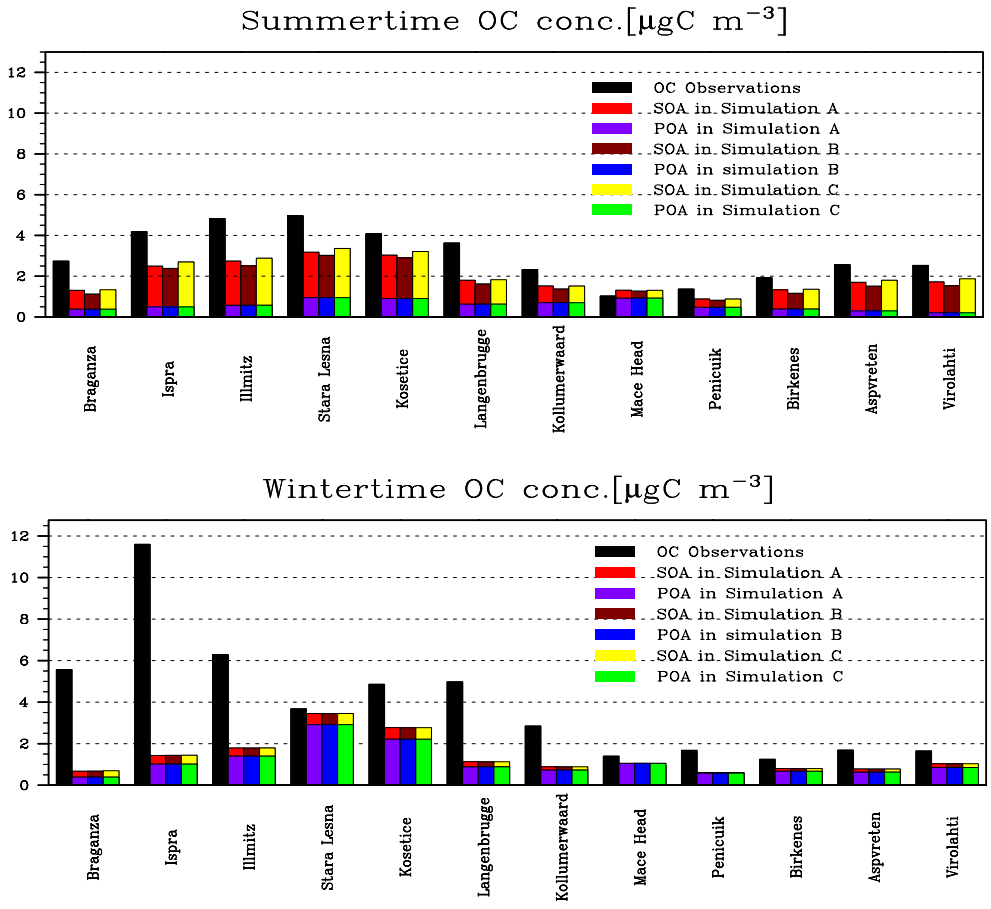

Fig. 6. OC concentrations in summer (July–October 2002 and April–July 2003) and winter (October 2002–April 2003) for 12 rural sites in the EMEP network. y-axis: OC concentration; The x-axis: site names (the sites are ordered according to latitude from the most southern station (left) to the the most northern station (right).

Table 8. Comparison of simulated seasonal average carbon concentrations (in μg C m^{-3}) with the observations made in Aveiro and K-Puszta from Gelencsér et al. (2007) and in Ispra from Gilardoni et al. (2011b).

Station Name	Source	Winter				Summer			
		Observation	Simulation A	Simulation B	Simulation C	Observations	Simulation A	Simulation B	Simulation C
Aveiro	POC_bb*	8.96	0.02	0.02	0.02	0.28	0.06	0.06	0.06
	POC_ff*	0.18	0.08	0.08	0.08	0.30	0.02	0.02	0.02
	SOC_bio*	0.70	0.10	0.10	0.11	2.54	0.29	0.22	0.29
	SOC_ff*	2.27	0.04	0.04	0.04	0.30	0.01	0.01	0.01
K-Puszta	POC_bb	4.30	0.01	0.01	0.01	0.32	0.03	0.03	0.03
	POC_ff	0.59	1.75	1.75	1.75	0.27	0.56	0.56	0.56
	SOC_bio	2.24	0.04	0.04	0.04	3.48	2.29	1.94	2.44
	SOC_ff	1.63	0.24	0.24	0.24	0.19	0.20	0.14	0.15
Ispra	POC_bb	11.9	0.02	0.02	0.02	0.5	0.04	0.04	0.04
	POC_ff	1.2	0.82	0.82	0.82	0.6	0.34	0.34	0.34
	SOC_bio	2.0	0.19	0.20	0.21	3.1	1.83	1.78	2.10
	SOC_ff	2.3	0.26	0.25	0.25	1.3	0.23	0.20	0.21

* POC_bb: primary organic carbon from biomass burning; POC_ff: primary organic carbon from fossil fuel and biofuel burning; SOC_bio: secondary organic carbon from the oxidation of biogenic species; SOC_ff: secondary organic carbon from fossil fuel and biofuel burning. Half of the POC burden is assumed to be composed of low-volatility compounds that may have undergone reactions and partitioned back into the aerosol form as SOA after emission.

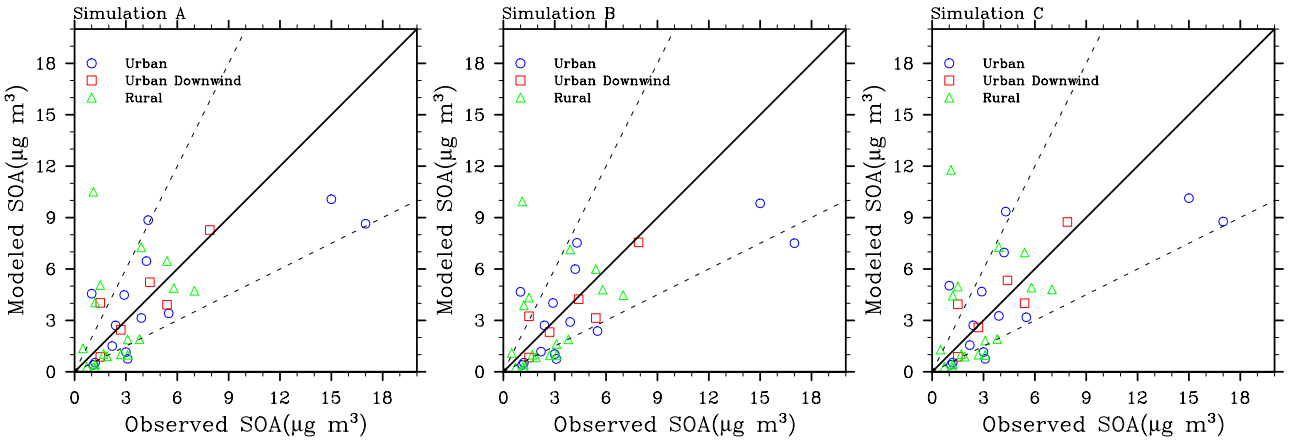

Fig. 7. Comparison of SOA mass concentrations observed at the urban, urban-downwind and rural sites reported in Zhang et al. (2007) with those simulated in Simulation A, Simulation B and Simulation C. Solid lines show the 1:1 ratio, and dashed lines show the 1:2 and 2:1 ratios. The measurements at the various sites were made in different seasons and different years between 2000 and 2006 and were reported for the average of varying durations spanning from 8 to 36 days. The model results are the average values over the same months as the observations.

of biogenic VOC emissions in these regions, by the low value of enthalpy that is used to represent the temperature dependence of gas-particle partitioning efficiency, by a wet scavenging rate that is too high, or by an underrepresentation of SOA formation from anthropogenic sources. It should nevertheless be emphasized that some of the EMEP stations, notably Ispra, are located in topographically pronounced terrain and represent rather localized conditions, which are difficult to quantitatively capture with a global model.

Zhang et al. (2007) present observational SOA data (measured by aerosol mass spectrometry, AMS) from a series of surface measurements at multiple sites in the Northern Hemisphere. The measurements at the various sites were made in different seasons and different years between 2000 and 2006 and were reported for the average of varying durations spanning from 8 to 36 days. In addition, most of the reported measurements were performed in urban locations. However, because of the unique nature of these measurements, all sites are included in our comparison though we differentiate the urban and downwind urban sites from rural sites. Figure 7 shows that the model underestimates the observations in urban locations, while it overestimates the measurements for rural sites and urban downwind sites. We do not expect the model with its low horizontal resolution to capture the POA emissions at urban sites, nor would we capture high local VOC and NO_x emissions, which have a very complex effect on SOA formation due to non-linear chemistry (Stroud et al., 2011). Nevertheless, the model-predicted SOA is subject to longer formation times than is POA, and is in reasonable agreement with the AMS observations. The NMB for Simulation A is −0.152, 0.058 and 0.157 for urban, urban downwind and rural sites, respectively (see the Table 7). The introduction of the Peeters et al. (2009) isoprene mechanism improves the agreement between predicted and observed SOA concentrations at rural sites giving an NMB of 0.065, but under-estimates the urban observations even more. The correlation coefficient for the rural sites in the AMS dataset is small, similar to the correlation coefficient for the IMPROVE sites.

The Zhang et al. (2007) database is limited to the Northern Hemisphere extra-tropics, which are influenced by both anthropogenic and biogenic sources. Observations from more remote forested regions may provide a more stringent test of the biogenic sources represented in the model. Table 9 shows measurements from three different campaigns in tropical forested areas in comparison with the model simulations corresponding to the location and time of measurements. While typical measurements in Northern Hemishpere mid latitudes indicate an average of about 2–3 μg m^{-3} for remote sites (Zhang et al., 2007), these forested regions show a relatively low loading of OM of only ∼1 μg m^{-3}. In contrast, the model predicts OM that is about a factor of 3 too high over both West Africa and the Amazon basin and a factor of 2 too high over Borneo, Malaysia. Chen et al. (2009) indicated that biogenic SOA dominated the submicron organic aerosol during the AMAZE 2008 experiment, consistent with our model findings. Therefore, it seems likely that either the production rate of SOA in the model is too large or the biogenic sources are too strong, although the prediction of POA at this site explains around 10 % of the total predicted OM. The introduction of the Peeters et al. (2009) HO_x-recycling mechanism improves the model estimate of isoprene, but actually degrades the comparison of OM by a small amount. It appears from these comparisons that the SOA formation mechanism (from, for example, the uptake of glyoxal, methyglyoxal and epoxide) in tropical forests needs to be improved. Amazon basin OC concentrations were also overestimated in the recent study of Gilardoni et al. (2011a), who investigated the

Table 9. Comparison of simulated OA with observed OA measured in tropical forested regions.

		Observations	Simulation A	Simulation B	Simulation C
West Africa (below 2 km)	Total OM ($\mu g\,m^{-3}$)	1.18 (Capes et al., 2009)	5.20	4.53	5.59
	POA* ($\mu g\,m^{-3}$)	–	0.57	0.57	0.57
	sv_oSOA ($\mu g\,m^{-3}$)	–	0.42	0.41	0.55
	ne_oSOA ($\mu g\,m^{-3}$)	–	0.70	0.51	0.79
	ne_GLYX ($\mu g\,m^{-3}$)	–	0.49	1.08	1.03
	ne_MGLY ($\mu g\,m^{-3}$)	–	1.59	1.45	1.63
	ne_IEPOX ($\mu g\,m^{-3}$)	–	1.43	0.51	1.02
	Isoprene (ppt)	620 (Capes et al., 2009)	1734	845	1126
	NOx (ppb)	0.21 (Capes et al., 2009)	0.34	0.37	0.35
Amazon basin (surface)	Total OM ($\mu g\,m^{-3}$)	0.70 (Chen et al., 2009)	3.55	3.82	4.45
		1.70 (Gilardoni et al., 2011a)			
	POA* ($\mu g\,m^{-3}$)	–	0.36	0.36	0.36
	sv_oSOA ($\mu g\,m^{-3}$)	–	0.28	0.36	0.46
	ne_oSOA ($\mu g\,m^{-3}$)	–	0.31	0.26	0.37
	ne_GLYX ($\mu g\,m^{-3}$)	–	0.24	0.95	0.87
	ne_MGLY ($\mu g\,m^{-3}$)	–	1.20	1.49	1.57
	ne_IEPOX ($\mu g\,m^{-3}$)	–	1.12	0.40	0.82
	Isoprene (ppb)	2.0 (Chen et al., 2009)	4.4	1.9	2.7
Malaysian Borneo (surface)	Total OM ($\mu g\,m^{-3}$)	0.74 (Robinson et al., 2011)	1.53	1.21	1.57
	POA* ($\mu g\,m^{-3}$)	–	0.25	0.25	0.25
	sv_oSOA ($\mu g\,m^{-3}$)	–	0.07	0.05	0.08
	ne_oSOA ($\mu g\,m^{-3}$)	–	0.08	0.06	0.09
	ne_GLYX ($\mu g\,m^{-3}$)	–	0.15	0.32	0.34
	ne_MGLY ($\mu g\,m^{-3}$)	–	0.45	0.40	0.47
	ne_IEPOX ($\mu g\,m^{-3}$)	–	0.53	0.13	0.34

* Half of the POA burden is assumed to be composed of low-volatility compounds that may have undergone reactions and partitioned back into the aerosol form as SOA after emission.

composition of fine and coarse aerosols in a Brazilian forest site from February through September 2008. Gilardoni et al. (2011a) reported average $PM_{2.5}$ OM concentrations during the wet season (February–June) of $1.7\,\mu g\,m^{-3}$, larger than the wet season concentrations measured at the same site by Chen et al. (2009) by about 60–80 %. In comparison with these measurements, our simulated concentrations are high by a factor of 2. The Gilardoni et al. (2011a) simulations were based on the TM5 global chemistry transport model and treat SOA as a primary species (i.e., they assumed that 15 %

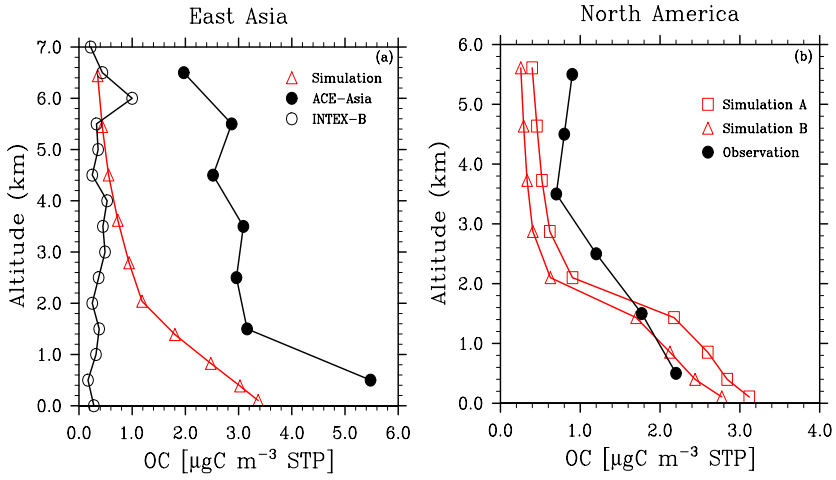

Fig. 8. Mean vertical profiles of total organic carbon at standard conditions of temperature and pressure. Observed mean profiles (black solid circles) were measured during the ACE-Asia campaign at Fukue Island off the coast of Japan in April/May 2001 (left plot) and during the ITCT-2K4 aircraft campaign over NE North America that took place in the Summer (July to August) 2004 (right plot). The black empty circles in the left plot represent average vertical profile of aerosol species for Asian pollution layers measured during the INTEX-B campaign made during April to May in 2006. The model results are the average values over the months of the campaigns. Three simulations produce very similar profiles over East Asia, thus only one simulated profile is shown in **(a)**. The vertical profile over North America produced in Simulation C is omitted because it is almost identical to that of Simulation A.

of natural terpene emissions form SOA and are directly emitted into the model atmosphere). Thus, these simulations also cannot capture observed OM in tropical regions.

The comparisons with the measurements reported above provide an evaluation of the model's ability to predict OA or OC mass distributions, but they do not evaluate the predicted chemical composition of the organic aerosol. There are very few speciated compounds that can be compared to the model, but organic functional groups in atmospheric particles have been measured by proton nuclear magnetic resonance (^{1}H-NMR) spectroscopy (Decesari et al., 2000), which provide some insight into the OA composition. Therefore, we compiled the data for measured functional groups reported in the literature and compare these to the relative contributions of different functional groups in the model predictions. We included the ^{1}H-NMR data measured in mid-latitudes in the warm season (Po Valley in spring and summer (Decesari et al., 2001), Mace Head (Ireland) from April to October for submicron WSOC (Cavalli et al., 2004), Jeju Island (Korea) during ACE-Asia (Decesari et al., 2005), and Hyyttiälä (Finland) in spring (Cavalli et al., 2006), i.e., under conditions in which SOA are expected to dominate. These data all show compositions with a high H-C (unfunctionalized alkyls) and HC-C=O (aliphatic carbons bound to an unsaturated carbon atom) content, which roughly accounts for 50 % and 35 % of the total WSOC mass, respectively. The model underestimates the contributions of these two functional groups in Simulation A, which predicts that the total SOA predicted in these regions consists of approximately 35 % of H-C, 10 % of HC-C=O, and 35 % of H-C=O (aldehyde). The introduction of the Peeters et al. (2009) HO_x recycling mechanism does not improve the prediction by very much and increases the fraction of the H-C=O group to about 40 %. Most of H-C=O group in the model comes from ne_GLYX and ne_MGLY, which we assumed had the same chemical structural as their gas-phase precursors for this comparison. This assumption may overestimate the contribution of H-C=O group and underestimate the contribution of HC-C=O group, because many laboratory studies have suggested that dissolved glyoxal and methylglyoxal will be oxidized by dissolved OH to carboxylic acids (e.g., glyoxylic, oxalic and pyruvic acid) in cloud and aerosol water (Ervens and Volkamer, 2010; Lim et al., 2010; Tan et al., 2010). Overall, the model can predict the measured H-C group to some extent, but, without further defining the chemistry of dissolved glyoxal and methylglyoxal, underestimates the relative abundance of the HC-C=O group and over-predicts the contribution of the H-C=O group.

4.2 Vertical profiles

Figure 8a compares the simulated mean vertical profile of OC concentrations and the observed mean profile measured by aircraft off the coast of Japan during the ACE-Asia campaign from April to May 2001. The measurements were made by two methods (thermal optical analysis and Fourier Transform infrared transmission spectroscopy) and were in excellent agreement (Maria et al., 2003). Heald et al. (2005) compared these measurements with the simulation from the GEOS-Chem global 3-D chemical transport model and deduced that a large source of organic aerosol in the free

troposphere is missing from current models. Here, we show the results of our model for the same month that the measurements were made, but for a different year and consequently with different meteorology than during the measurements. Figure 8a shows that there are still large discrepancies between the model and the measurements in the free troposphere, although the magnitude of the discrepancy is smaller than that reported by Heald et al. (2005) (10–100 times). Dunlea et al. (2009) examined the evolution of Asian aerosols during transpacific transport in the INTEX-B campaign and found no evidence for significant SOA formation in the free troposphere. The AMS aircraft measurements for Asian pollution layers in the INTEX-B campaign were about an order of magnitude lower than those measured during the ACE-Asia campaign, and our results compare favorably with the INTEX-B results at altitudes higher than 3 km. Similarly, the aircraft observations during the ITCT-2K4 aircraft campaign, conducted from 9 July to 15 August 2004 out of Portsmouth, New Hampshire, did not suggest a major SOA source in the free troposphere either (Heald et al., 2006). An illustrative comparison of the vertical profile of values from our model for aerosol OC with the measured water-soluble organic carbon (WSOC) from the Particle-Into-Liquid Sampler (PILS) instrument on board the NOAA WP3 aircraft is shown in Fig. 8b. The model performs reasonably well in the boundary layer (below 2 km), but still underestimates OC in the free troposphere (2–6 km). The mean observed concentration was $0.900 \pm 0.187\,\mu g\,C\,m^{-3}$ in the free troposphere (Heald et al., 2006), while the corresponding mean model value in Simulation A is $0.574 \pm 0.172 \mu g\,C\,m^{-3}$.

5 Sensitivity tests of the oligomer formation rate

As discussed in Sect. 2.2.1, the rate formation of oligomers in heterogeneous reactions within aerosols may vary with different compounds and with the concentration of semivolatile compounds within the aerosols. Therefore, two extra simulations were performed using the same chemical mechanism as used in Simulation C but with a lifetime for oligomer formation of 2 days and 0.5 days, respectively. As expected, the shorter lifetime enhances the transfer from condensed SVOCs to oligomers, which increases the burden of ne_oSOA by 0.15 Tg (23 %) in comparison with the burden obtained in Simulation C. Correspondingly, the burden of ne_oSOA in the simulation using a lifetime for the formation of oligomers of 2 days is decreased by 0.19 Tg (28 %). The short lifetime of 0.5 days increases the gap between the annual mean simulation and the observations in IMPROVE network, and results in a normalized mean bias (NMB) of 10.3 % compared to the NMB of 1.7 % in Simulation C. In addition, the shorter lifetime increases the NMB between the simulation and AMS observations slightly, i.e., from −12.5 % to −5.5 % at urban sites, from 8.9 % to 20.9 % at urban downwind sites, and from 20.0 % to 27.0 % at rural sites. In contrast, the 2-day lifetime decreases the NMB to −16.5 % at urban sites, to 1.9 % at urban downwind sites and to 15.0 % at rural sites, and produces a simulation with a NMB of −3.4 % compared to the annual mean observations from IMPROVE network. The 0.5-day lifetime brings the simulation slightly closer to the EMEP observations in terms of NMB compared to the 1-day lifetime, but the simulation still under-estimates the observations by over 50 %. While the change of the lifetime has an effect on the NMB values, there are only small changes to the correlation coefficients (R) between the simulations and various observations. At the three tropical sites, the ne_oSOA component only explains a small part of the total OA, so the change in the lifetime for the formation of oligomers causes only a very small change in the total OA (4 %). Therefore, these simulations still over-predict the measurements by more than a factor of 2. Similarly, the vertical profiles of OC off of East Asia and over North America are almost the same as those shown above.

6 Discussion and conclusions

The IMPACT model was used to simulate global SOA formation using three different mechanisms. We accounted for SOA formation from traditional gas-particle partitioning using an explicit full chemistry scheme instead of a 2-product model that has been used in a number of previous studies. These condensed SVOCs are assumed to go undergo further aerosol-phase reactions to form oligomers with a fixed time constant (assumed to be 1 day in the baseline model). We also included SOA formation from the uptake of gas-phase glyoxal and methlyglyoxal onto clouds and aqueous sulfate aerosol following the work of Fu et al. (2008, 2009), and from the uptake of gas-phase epoxides onto aqueous sulfate aerosol following the work of Paulot et al. (2009). In addition, we examined the influence of including the HO_x recycling mechanism proposed by Peeters et al. (2009) for the oxidation of isoprene. Our SOA formation mechanisms were evaluated by comparing our global chemical transport model simulations with surface observations from the IMPROVE network in North America, the EMEP network in Europe and from a collection of AMS measurements. We also compared our results with vertical profiles of OC from aircraft measurements off of East Asia and over North America.

The total SOA source in Simulation A was $115.7\,Tg\,yr^{-1}$, much larger than that estimated by previous global chemical transport models (see Table 5), but is within the range of recent top-down estimates that use satellite observations and AMS measurements (Heald et al., 2010; Spracklen et al., 2011). The SOA formation from biogenic precursors (e.g., isoprene, monoterpenes, etc.) dominates those from anthropogenic sources by a large margin, i.e., the fraction of biogenic SOA is 88 %. However, the production of "biogenic" SOA is strongly linked with anthropogenic

components through a variety of mechanisms. Thus, anthropogenic POA emissions provide an absorptive medium for the condensation of semivolatile species of biogenic origin, and anthropogenic sulfate aerosols facilitate the conversion of glyoxal, methlyglyoxal and epoxides of biogenic origin to SOA. The formation of SOA from biogenic VOCs is also influenced by anthropogenic emissions of NO_x, not only because these biogenic VOCs react with anthropogenic NO_x or NO_3 to form SVOCs (e.g., isoprene-hydroxy-nitrate), but also because NO_x competes with HO_2 for peroxy radicals formed in the initial stages of VOC oxidation (e.g., Reactions R1 and R3), leading to changes in functional groups and affecting subsequent reactions. The feedback between anthropogenic emissions and the formation of SOA from biogenic VOCs could have significant implications for future emissions regulations and for predicting the change of organic aerosol in response to future climate change. In order to control emissions contributing to the organic aerosol burden, it is necessary to separate the anthropogenic contribution to SOA formation from the natural background OA (Hoyle et al., 2011).

The introduction of the Peeters et al. (2009) HO_x recycling mechanism into the isoprene oxidation scheme has a strong impact on global SOA formation. It decreases the production rate of ne_oSOA, ne_MGLY and ne_IEPOX by about 28 %, 16 % and 65 %, respectively, as a result of the competition between the unimolecular isomerization pathway and the traditional oxidation pathways, i.e., isoprene $RO_2 + NO$ and isoprene $RO_2 + HO_2$. On the other hand, it increases the SOA production rates from glyoxal by about 65 %. The combination of these effects causes the total SOA source to only decrease by 25 %. When the reaction rates for the 1,5-H and 1,6-H shifts in isoprene radicals are decreased by a factor of 10, the total SOA production rate increases from 87 Tg yr^{-1} to 113 Tg yr^{-1}, very close to that from simulation A which does not consider the HO_x recycling mechanism. The large difference between the Simulations B and C is indicative of the discrepancy between state-of-the-art density functional theories (Peeters et al., 2009) and laboratory measurements (Crounse et al., 2011). These different SOA production rates imply that further laboratory studies, field measurements and theoretical studies are needed to better constrain the budgets of the SOA components.

Comparison with the IMPROVE network and with AMS surface measurements in the Northern Hemisphere shows that the model can predict the surface organic aerosol concentrations reasonably well with low normalized mean biases ranging from −15 % to 15 % in rural regions. The low normalized mean biases for the IMPROVE network and AMS surface measurements contrasts with the under-predictions of observations by other models (Chung and Seinfeld, 2002; Liao et al., 2007; Farina et al., 2010; Utembe et al., 2011; Yu, 2011). The low correlation coefficients R (varying from 0.3 to 0.5) between the simulations and observations, however, indicate that the model does not capture the spatial variability of the measurements very well. These may be compared to the correlation coefficients R of around 0.65 between simulations and observations for the IMPROVE network reported in other models (Park et al., 2003; Liao et al., 2007; Farina et al., 2010). The comparison with the EMEP measurements demonstrates that the model under-predicts surface OC concentrations in Europe, which may be the result of an underestimation of POA in winter and of SOA in summer. In pristine tropical forest regions, the model overestimates the OM burden by roughly a factor of three compared to three surface AMS measurements made in West Africa, Amazon and Malaysia. This overestimation is present both with and without the HO_x recycling mechanism in the isoprene oxidation scheme. Our overestimation in the Amazon basin differs significantly from predictions of the GEOS-Chem model, which underestimated OM (Chen et al., 2009), but is consistent with the TM5 model over-prediction (Gilardoni et al., 2011a). Because the ne_GLYX, ne_MGLY and ne_IEPOX components account for the major fraction of total OM predicted at these sites (Table 9), it is important to improve the formation of these compounds in the model. Trainic et al. (2011) conducted experiments to study the uptake of glyoxal on ammonium sulfate seed aerosols under hydrated conditions over a wide range of relative humidities (RH from 35 % to 90 %) and found that the reactive uptake rate decreased with increasing RH. The ratio of the final organic aerosol mass to the seed mass at the 50 % RH condition was similar to that found by Liggio et al. (2005a) (who conducted their studies at 49 % RH), but decreased by 57 % when the RH increased to 90 %. This trend was attributed to the slower glyoxal oligomerization rate caused by the dilution of the ammonium sulfate aerosol at the higher RH values (Liggio et al., 2005a; Trainic et al., 2011). Thus, the work of Trainic et al. (2011) may indicate that the uptake coefficient adopted here for sulfate aerosols (which was based on Liggio et al., 2005a) as well as its application to cloud water is too high in much of the tropics where typical RH values are around 90 %. In addition, the simple treatment of irreversible surface controlled uptake might be misleading if there is a competition between reversible vs. irreversible uptake and of bulk reactions vs. surface processes (Ervens and Volkamer, 2010). Furthermore, the same uptake coefficient for both cloud droplets and aqueous aerosols cannot account for the differences in the chemistry of carbonyl compounds between cloud water and aerosol water (Lim et al., 2010; Ervens and Volkamer, 2010). Therefore, it may be that improvements to the processes responsible for the formation of SOA from glyoxal, methylglyoxal and epoxide would improve the model. Given the sparse amount of data, however, the conclusion that the model overestimates surface OM concentrations observed at 3 sites in the tropical forest regions may not necessarily lead to the conclusion that the model is in error. It would be valuable to have more measurements and model studies to examine the properties of organic aerosols in the tropics. In the free troposphere, the model reproduces the OC

observed during the ITCT-2K4 aircraft campaign over North America relatively well, but clearly underestimates OC observations during ACE-Asia campaign off the coast of Japan. However, the model simulates Asian pollution layers above 3 km during the INTEX-B campaign very well.

Supplementary material related to this article is available online at: http://www.atmos-chem-phys.net/12/4743/2012/acp-12-4743-2012-supplement.pdf.

Acknowledgements. This project was supported by the EPA STAR program (grant #83337701). The research leading to these results has received funding from the European Research Council under the European Union's Seventh Framework Programme (FP7/2007-2013)/ERC grant agreement no 226144. Any opinions, findings, and conclusions or recommendations expressed in this material are those of the authors and do not necessarily reflect the views of the EPA. We thank Roy Chen for his critical help with porting the model code to different computers and help in implementing the graphics codes.

Edited by: M. Schulz

References

Abdul-Razzak, H. and Ghan, S. J.: A parameterization of aerosol activation 2. Multiple aerosol types, J. Geophys. Res., 105, 6837–6844, 2000.

Abdul-Razzak, H. and Ghan, S. J.: A parameterization of aerosol activation – 3. Sectional representation, J. Geophys. Res., 107, 4026, doi:10.1029/2001JD000483, 2002.

Archibald, A. T., Cooke, M. C., Utembe, S. R., Shallcross, D. E., Derwent, R. G., and Jenkin, M. E.: Impacts of mechanistic changes on HO_x formation and recycling in the oxidation of isoprene, Atmos. Chem. Phys., 10, 8097–8118, doi:10.5194/acp-10-8097-2010, 2010.

Barley, M. H. and McFiggans, G.: The critical assessment of vapour pressure estimation methods for use in modelling the formation of atmospheric organic aerosol, Atmos. Chem. Phys., 10, 749–767, doi:10.5194/acp-10-749-2010, 2010.

Bessagnet, B., Seigneur, C., and Menut, L.: Impact of dry deposition of semi-volatile organic compounds on secondary organic aerosols, Atmos. Environ., 44, 1781–1787, 2010.

Bey, I., Jacob, D., Yantosca, R., Logan, J., Field, B., Fiore, A., Li, Q., Liu, H., Mickley, L., and Schultz, M.: Global modeling of tropospheric chemistry with assimilated meteorology: Model description and evaluation, J. Geophys. Res., 106, 23073–23096, doi:10.1029/2001JD000807, 2001.

Bilde, M. and Pandis, S. N.: Evaporation rates and vapor pressures of individual aerosol species formed in the atmospheric oxidation of alpha- and beta-pinene, Environ. Sci. Technol., 35, 3344–3349, 2001.

Blando, J. D. and Turpin, B. J.: Secondary organic aerosol formation in cloud and fog droplets: a literature evaluation of plausibility, Atmos. Environ., 34, 1623–1632, 2000.

Booth, A. M., Barley, M. H., Topping, D. O., McFiggans, G., Garforth, A., and Percival, C. J.: Solid state and sub-cooled liquid vapour pressures of substituted dicarboxylic acids using Knudsen Effusion Mass Spectrometry (KEMS) and Differential Scanning Calorimetry, Atmos. Chem. Phys., 10, 4879–4892, doi:10.5194/acp-10-4879-2010, 2010.

Booth, A. M., Montague, W. J., Barley, M. H., Topping, D. O., McFiggans, G., Garforth, A., and Percival, C. J.: Solid state and sub-cooled liquid vapour pressures of cyclic aliphatic dicarboxylic acids, Atmos. Chem. Phys., 11, 655–665, doi:10.5194/acp-11-655-2011, 2011.

Bowman, F. M. and Karamalegos, A. M.: Estimated effects of composition on secondary organic aerosol mass concentrations, Environ. Sci. Technol., 36, 2701–2707, 2002.

Butler, T. M., Taraborrelli, D., Brühl, C., Fischer, H., Harder, H., Martinez, M., Williams, J., Lawrence, M. G., and Lelieveld, J.: Improved simulation of isoprene oxidation chemistry with the ECHAM5/MESSy chemistry-climate model: lessons from the GABRIEL airborne field campaign, Atmos. Chem. Phys., 8, 4529–4546, doi:10.5194/acp-8-4529-2008, 2008.

Camredon, M. and Aumont, B.: Assessment of vapor pressure estimation methods for secondary organic aerosol modeling, Atmos. Environ., 40, 2105–2116, 2006.

Camredon, M., Aumont, B., Lee-Taylor, J., and Madronich, S.: The SOA/VOC/NO_x system: an explicit model of secondary organic aerosol formation, Atmos. Chem. Phys., 7, 5599–5610, doi:10.5194/acp-7-5599-2007, 2007.

Camredon, M., Hamilton, J. F., Alam, M. S., Wyche, K. P., Carr, T., White, I. R., Monks, P. S., Rickard, A. R., and Bloss, W. J.: Distribution of gaseous and particulate organic composition during dark α-pinene ozonolysis, Atmos. Chem. Phys., 10, 2893–2917, doi:10.5194/acp-10-2893-2010, 2010.

Capes, G., Murphy, J. G., Reeves, C. E., McQuaid, J. B., Hamilton, J. F., Hopkins, J. R., Crosier, J., Williams, P. I., and Coe, H.: Secondary organic aerosol from biogenic VOCs over West Africa during AMMA, Atmos. Chem. Phys., 9, 3841–3850, doi:10.5194/acp-9-3841-2009, 2009.

Cappa, C. D. and Jimenez, J. L.: Quantitative estimates of the volatility of ambient organic aerosol, Atmos. Chem. Phys., 10, 5409–5424, doi:10.5194/acp-10-5409-2010, 2010.

Carlton, A. G., Turpin, B. J., Altieri, K. E., Seitzinger, S., Reff, A., Lim, H. J., and Ervens, B.: Atmospheric oxalic acid and SOA production from glyoxal: Results of aqueous photooxidation experiments, Atmos. Environ., 41, 7588–7602, 2007.

Carlton, A. G., Pinder, R. W., Bhave, P. V., and Pouliot, G. A.: To what extent can biogenic SOA be controlled?, Environ. Sci. Technol., 44, 3376–3380, 2010.

Cavalli, F., Facchini, M. C., Decesari, S., Mircea, M., Emblico, L., Fuzzi, S., Ceburnis, D., Yoon, Y. J., O'Dowd, C., Putaud, J.-P., and Dell'Acqua, A.: Advances in characterization of size-resolved organic matter in marine aerosol over the North Atlantic, J. Geophys. Res., 109, D24215, doi:10.1029/2004JD005137, 2004.

Cavalli, F., Facchini, M. C., Decesari, S., Emblico, L., Mircea, M., Jensen, N. R., and Fuzzi, S.: Size-segregated aerosol chemical composition at a boreal site in southern Finland, during the QUEST project, Atmos. Chem. Phys., 6, 993–1002, doi:10.5194/acp-6-993-2006, 2006.

Chan, A. W. H., Kroll, J. H., Ng, N. L., and Seinfeld, J. H.: Kinetic modeling of secondary organic aerosol formation: effects of particle- and gas-phase reactions of semivolatile products, Atmos. Chem. Phys., 7, 4135–4147, doi:10.5194/acp-7-4135-2007, 2007.

Chan, M. N., Surratt, J. D., Claeys, M., Edgerton, E. S., Tanner, R. L., Shaw, S. L., Zheng, M., Knipping, E. M., Eddingsaas, N. C., Wennberg, P. O., and Seinfeld, J. H.: Characterization and quantification of isoprene-derived epoxydiols in ambient aerosol in the southeastern United States, Environ. Sci. Technol., 44, 4590–4596, doi:10.1021/es100596b, 2010.

Chen, Q., Farmer, D. K., Schneider, J., Zorn, S. R., Heald, C. L., Karl, T. G., Guenther, A., Allan, J. D., Robinson, N., Coe, H., Kimmel, J. R., Pauliquevis, T., Borrmann, S., Pöschl, U., Andreae, M. O., Artaxo, P., Jimenez, J. L., and Martin, S. T.: Mass spectral characterization of submicron biogenic organic particles in the Amazon Basin, Geophys. Res. Lett., 36, L20806, doi:10.1029/2009gl039880, 2009.

Chung, S. H. and Seinfeld, J. H.: Global distribution and climate forcing of carbonaceous aerosols, J. Geophys. Res., 107, D19, doi:10.1029/2001jd001397, 2002.

Claeys, M., Graham, B., Vas, G.,Wang, W., Vermeylen, R., Pashynska, V., Cafmeyer, J., Guyon, P., Andreae, M. O., Artaxo, P., and Maenhaut, W.: Formation of secondary organic aerosols through photooxidation of isoprene, Science, 303, 1173–1176, 2004.

Coy, L. and Swinbank, R.: Characteristics of stratospheric winds and temperatures produced by data assimilation, J. Geophys. Res., 102, 25763–25781, 1997.

Coy, L., Nash, E. R., and Newman, P. A.: Meteorology of the polar vortex: Spring 1997, Geophys. Res. Lett., 24, 2693–2696, 1997.

Crounse, J. D., Paulot, F., Kjaergaard, H. G., and Wennberg, P. O.: Peroxy radical isomerization in the oxidation of isoprene, Phys. Chem. Chem. Phys., 13, 13607–13613, 2011.

Czoschke, N. M., Jang, M., and Kamens, R. M.: Effect of acidic seed on biogenic secondary organic aerosol growth, Atmos. Environ., 37, 4287–4299, 2003.

Da Silva, G., Graham, C., and Wang, Z.-F.: Unimolecular β-hydroxyperoxy radical decomposition with OH recycling in thephotochemical oxidation of isoprene, Environ. Sci. Technol., 44, 250–256, 2010.

Decesari, S., Facchini, M. C., and Fuzzi, S.: Characterization of water-soluble organic compounds in atmospheric aerosols: a new approach, J. Geophys. Res., 105, 1481–1489, 2000.

Decesari, S., Facchini, M. C., Matta, E., Lettini, F., Mircea, M., Fuzzi, S., Tagliavini, E., and Pautaud, J.-P.: Chemical features and seasonal variation of fine aerosol water-soluble organic compounds in the Po Valley, Italy, Atmos. Environ., 35, 3691–3699, 2001.

Decesari, S., Facchini, M. C., Fuzzi, S., McFiggans, G. B., Coe, H., and Bower, K. N.: The water-soluble organic component of size-segregates aerosol, cloud water and wet depositions from Jeju Island during ACE-Asia, Atmos. Environ., 39, 211–222, 2005.

de Gouw, J. A., Middlebrook, A. M., Warneke, C., Goldan, P. D., Kuster, W. C., Roberts, J. M., Fehsenfeld, F. C., Worsnop, D. R., Canagaratna, M. R., Pszenny, A. A. P., Keene, W. C., Marchewka, M., Bertman, S. B., and Bates, T. S.: Budget of organic carbon in a polluted atmosphere: Results from the New England Air Quality Study in 2002, J. Geophys. Res., 110, D16, doi:10.1029/2004jd005623, 2005.

Dommen, J., Metzger, A., Duplissy, J., Kalberer, M., Alfarra, M. R., Gascho, A., Weingartner, E., Prevot, A. S. H., Verheggen, B., and Baltensperger, U.: Laboratory observation of oligomers in the aerosol from isoprene/NO_x photooxidation, Geophys. Res. Lett., 33, L13805, doi:10.1029/2006GL026523, 2006.

Donahue, N. M., Robinson, A. L., Stanier, C. O., and Pandis, S. N.: Coupled partitioning, dilution, and chemical aging of semivolatile organics, Environ. Sci. Technol., 40, 2635–2643, 2006.

Donahue, N. M., Robinson, A. L., and Pandis, S. N.: Atmospheric organic particulate matter: From smoke to secondary organic aerosol, Atmos. Environ., 43, 94–106, 2009.

Dunlea, E. J., DeCarlo, P. F., Aiken, A. C., Kimmel, J. R., Peltier, R. E., Weber, R. J., Tomlinson, J., Collins, D. R., Shinozuka, Y., McNaughton, C. S., Howell, S. G., Clarke, A. D., Emmons, L. K., Apel, E. C., Pfister, G. G., van Donkelaar, A., Martin, R. V., Millet, D. B., Heald, C. L., and Jimenez, J. L.: Evolution of Asian aerosols during transpacific transport in INTEX-B, Atmos. Chem. Phys., 9, 7257–7287, doi:10.5194/acp-9-7257-2009, 2009.

Dzepina, K., Volkamer, R. M., Madronich, S., Tulet, P., Ulbrich, I. M., Zhang, Q., Cappa, C. D., Ziemann, P. J., and Jimenez, J. L.: Evaluation of recently-proposed secondary organic aerosol models for a case study in Mexico City, Atmos. Chem. Phys., 9, 5681–5709, doi:10.5194/acp-9-5681-2009, 2009.

Eddingsaas, N. C., VanderVelde, D. G., and Wennberg, P. O.: Kinetics and products of the acid-catalyzed ring-opening of atmospherically relevant butyl epoxy alcohols, J. Phys. Chem. A, 114, 8106–8113, 2010.

Epstein, S., Riipinen, I., and Donahue, A. M.: A semiempirical correlation between enthalpy of vaporization and saturation concentrationfor organic aerosol, Environ. Sci. Technol., 44, 743–748, 2010.

Ervens, B. and Volkamer, R.: Glyoxal processing by aerosol multiphase chemistry: towards a kinetic modeling framework of secondary organic aerosol formation in aqueous particles, Atmos. Chem. Phys., 10, 8219–8244, doi:10.5194/acp-10-8219-2010, 2010.

Farina, S. C., Adams, P. J., and Pandis, S. N.: Modeling global secondary organic aerosol formation and processing with the volatility basis set: Implications for anthropogenic secondary organic aerosol, J. Geophys. Res., 115, D09202, doi:10.1029/2009JD013046, 2010.

Froyd, K. D., Murphy, S. M., Murphy, D. M., de Gouw, J. A., Eddingsaas, N. C., and Wennberg, P. O.: Contribution of isoprene-derived organosulfates to free tropospheric aerosol mass, P. Natl. Acad. Sci. USA, 107, 21360–21365, 2010.

Fu, T. M., Jacob, D. J., Wittrock, F., Burrows, J. P., Vrekoussis, M., and Henze, D. K.: Global budgets of atmospheric glyoxal and methylglyoxal, and implications for formation of secondary organic aerosols, J. Geophys. Res., 113, D15303, doi:10.1029/2007JD009505, 2008.

Fu, T. M., Jacob, D. J., and Heald, C. L.: Aqueous-phase reactive uptake of dicarbonyls as a source of organic aerosol over eastern North America, Atmos. Environ., 43, 1814–1822, 2009.

Galloway, M. M., Chhabra, P. S., Chan, A. W. H., Surratt, J. D., Flagan, R. C., Seinfeld, J. H., and Keutsch, F. N.: Glyoxal uptake on ammonium sulphate seed aerosol: reaction products and reversibility of uptake under dark and irradiated conditions,

Atmos. Chem. Phys., 9, 3331–3345, doi:10.5194/acp-9-3331-2009, 2009.

Gantt, B., Meskhidze, N., and Kamykowski, D.: A new physically-based quantification of marine isoprene and primary organic aerosol emissions, Atmos. Chem. Phys., 9, 4915–4927, doi:10.5194/acp-9-4915-2009, 2009.

Gao, S., Keywood, M., Ng, N. L., Surratt, J., Varutbangkul, V., Bahreini, R., Flagan, R. C., and Seinfeld, J. H.: Low-molecular-weight and oligomeric components in secondary organic aerosol from the ozonolysis of cycloalkenes and alpha-pinene, J. Phys. Chem. A, 108, 10147–10164, 2004a.

Gao, S., Ng, N. L., Keywood, M., Varutbangkul, V., Bahreini, R., Nenes, A., He, J. W., Yoo, K. Y., Beauchamp, J. L., Hodyss, R. P., Flagan, R. C., and Seinfeld, J. H.: Particle phase acidity and oligomer formation in secondary organic aerosol, Environ. Sci. Technol., 38, 6582–6589, 2004b.

Gelencsér, A., Hoffer, A., Krivacsy, Z., Kiss, G., Molnar, A., and Meszaros, E.: On the possible origin of humic matter in fine continental aerosol, J. Geophys. Res., 107, 4137, doi:10.1029/2001JD001299, 2002.

Gelencsér, A., May, B., Simpson, D., Sánchez-Ochoa, A., Kasper-Giebl, A., Puxbaum, H., Caseiro, A., Pio, C., and Legrand., M.: Source apportionment of $PM_{2.5}$ organic aerosol over Europe: Primary/secondary, natural/anthropogenic, and fossil/biogenic origin, J. Geophys. Res., 112, D23S04, doi:10.1029/2006JD008094, 2007.

Gilardoni, S., Vignati, E., Cavalli, F., Putaud, J. P., Larsen, B. R., Karl, M., Stenström, K., Genberg, J., Henne, S., and Dentener, F.: Better constraints on sources of carbonaceous aerosols using a combined ^{14}C – macro tracer analysis in a European rural background site, Atmos. Chem. Phys., 11, 5685–5700, doi:10.5194/acp-11-5685-2011, 2011a.

Gilardoni, S., Vignati, E., Marmer, E., Cavalli, F., Belis, C., Gianelle, V., Loureiro, A., and Artaxo, P.: Sources of carbonaceous aerosol in the Amazon basin, Atmos. Chem. Phys., 11, 2747–2764, doi:10.5194/acp-11-2747-2011, 2011b.

Giorgi, F. and Chameides, W. L.: Rainout lifetimes of highly soluble aerosols and gases as inferred from simulations with a g general-circulation model, J. Geophys. Res., 91, 14367–14376, 1986.

Goldstein, A. H. and Galbally, I. E.: Known and unexplored organic constituents in the earth's atmosphere, Environ. Sci. Technol., 41, 1514–1521, 2007.

Goldstein, A. H., Koven, C. D., Heald, C. L., and Fung, I. Y.: Biogenic carbon and anthropogenic pollutants combine to form a cooling haze over the southeastern United States, P. Natl. Acad. Sci. USA, 106, 8835–8840, 2009.

Gondwe, M., Krol, M., Klaassen, W., Gieskes, W., and de Baar, H.: The contribution of ocean-leaving DMS to the global atmospheric burdens of DMS, MSA, SO_2 and nss $SO_4^=$, Global Biogeochem. Cy., 17, 1056, doi:10.1029/2002GB001937, 2003

Griffin, R. J., Dabdub, D., and Seinfeld, J. H.: Secondary organic aerosol – 1. Atmospheric chemical mechanism for production of molecular constituents, J. Geophys. Res., 107, D17, doi:10.1029/2001JD000541, 2002.

Gross, D. S., Galli, M. E., Kalberer, M., Prevot, A. S. H., Dommen, J., Alfarra, M. R., Duplissy, J., Gaeggeler, K., Gascho, A., Metzger, A., and Baltensperger, U.: Real-time measurement of oligomeric species in secondary organic aerosol with the aerosol time-of-flight mass spectrometer, Anal. Chem., 78, 2130–2137, 2006.

Guenther, A., Hewitt, C. N., Erickson, D., Fall, R., Geron, C., Graedel, T., Harley, P., Klinger, L., Lerdau, M., McKay, W. A., Pierce, T., Scholes, B., Steinbrecher, R., Tallamraju, R., Taylor, J., and Zimmerman, P.: A global-model of natural volatile organic-compound emissions, J. Geophys. Res., 100, 8873–8892, 1995.

Guenther, A., Karl, T., Harley, P., Wiedinmyer, C., Palmer, P. I., and Geron, C.: Estimates of global terrestrial isoprene emissions using MEGAN (Model of Emissions of Gases and Aerosols from Nature), Atmos. Chem. Phys., 6, 3181–3210, doi:10.5194/acp-6-3181-2006, 2006.

Hallquist, M., Wenger, J. C., Baltensperger, U., Rudich, Y., Simpson, D., Claeys, M., Dommen, J., Donahue, N. M., George, C., Goldstein, A. H., Hamilton, J. F., Herrmann, H., Hoffmann, T., Iinuma, Y., Jang, M., Jenkin, M. E., Jimenez, J. L., Kiendler-Scharr, A., Maenhaut, W., McFiggans, G., Mentel, Th. F., Monod, A., Prévôt, A. S. H., Seinfeld, J. H., Surratt, J. D., Szmigielski, R., and Wildt, J.: The formation, properties and impact of secondary organic aerosol: current and emerging issues, Atmos. Chem. Phys., 9, 5155–5236, doi:10.5194/acp-9-5155-2009, 2009.

Hastings, W. P., Koehler, C. A., Bailey, E. L., and De Haan, D. O.: Secondary organic aerosol formation by glyoxal hydration and oligomer formation: Humidity effects and equilibrium shifts during analysis, Environ. Sci. Technol., 39, 8728–8735, 2005.

Heald, C. L., Jacob, D. J., Park, R. J., Russell, L. M., Huebert, B. J., Seinfeld, J. H., Liao, H., and Weber, R. J.: A large organic aerosol source in the free troposphere missing from current models, Geophys. Res. Lett., 32, L18809, doi:10.1029/2005GL023831, 2005.

Heald, C. L., Jacob, D. J., Turquety, S., Hudman, R. C., Weber, R. J., Sullivan, A. P., Peltier, R. E., Atlas, E. L., de Gouw, J. A., Warneke, C., Holloway, J. S., Neuman, J. A., Flocke, F. M., and Seinfeld, J. H.: Concentrations and sources of organic carbon aerosols in the free troposphere over North America, J. Geophys. Res., 111, D23S47, doi:10.1029/2006JD007705, 2006.

Heald, C. L., Henze, D. K., Horowitz, L. W., Feddema, J., Lamarque, J. F., Guenther, A., Hess, P. G., Vitt, F., Seinfeld, J. H., Goldstein, A. H., and Fung, I.: Predicted change in global secondary organic aerosol concentrations in response to future climate, emissions, and land use change, J. Geophys. Res., 113, D05211, doi:10.1029/2007JD009092, 2008.

Heald, C. L., Ridley, D. A., Kreidenweis, S. M., and Drury, E. E.: Satellite observations cap the atmospheric organic aerosol budget, Geophys. Res. Lett., 37, L24808, doi:10.1029/2010GL045095, 2010.

Heaton, K. J., Dreyfus, M. A., Wang, S., and Johnston, M. V.: Oligomers in the early stage of biogenic secondary organic aerosol formation and growth, Environ. Sci. Technol., 41, 6129–6136, 2007.

Henze, D. K. and Seinfeld, J. H.: Global secondary organic aerosol from isoprene oxidation, Geophys. Res. Lett., 33, L09812, doi:10.1029/2006GL025976, 2006.

Henze, D. K., Seinfeld, J. H., Ng, N. L., Kroll, J. H., Fu, T.-M., Jacob, D. J., and Heald, C. L.: Global modeling of secondary organic aerosol formation from aromatic hydrocarbons: high- vs. low-yield pathways, Atmos. Chem. Phys., 8, 2405–2420, doi:10.5194/acp-8-2405-2008, 2008.

Herzog, M., Weisenstein, D. K., and Penner, J. E.: A dynamic aerosol module for global chemical transport models: Model description, J. Geophys. Res., 109, D18202, doi:10.1029/2003JD004405, 2004.

Hodzic, A., Jimenez, J. L., Madronich, S., Canagaratna, M. R., DeCarlo, P. F., Kleinman, L., and Fast, J.: Modeling organic aerosols in a megacity: potential contribution of semi-volatile and intermediate volatility primary organic compounds to secondary organic aerosol formation, Atmos. Chem. Phys., 10, 5491–5514, doi:10.5194/acp-10-5491-2010, 2010.

Hoyle, C. R., Berntsen, T., Myhre, G., and Isaksen, I. S. A.: Secondary organic aerosol in the global aerosol – chemical transport model Oslo CTM2, Atmos. Chem. Phys., 7, 5675–5694, doi:10.5194/acp-7-5675-2007, 2007.

Hoyle, C. R., Myhre, G., Berntsen, T. K., and Isaksen, I. S. A.: Anthropogenic influence on SOA and the resulting radiative forcing, Atmos. Chem. Phys., 9, 2715–2728, doi:10.5194/acp-9-2715-2009, 2009.

Hoyle, C. R., Boy, M., Donahue, N. M., Fry, J. L., Glasius, M., Guenther, A., Hallar, A. G., Huff Hartz, K., Petters, M. D., Petäjä, T., Rosenoern, T., and Sullivan, A. P.: A review of the anthropogenic influence on biogenic secondary organic aerosol, Atmos. Chem. Phys., 11, 321–343, doi:10.5194/acp-11-321-2011, 2011.

Huffman, J. A., Docherty, K. S., Aiken, A. C., Cubison, M. J., Ulbrich, I. M., DeCarlo, P. F., Sueper, D., Jayne, J. T., Worsnop, D. R., Ziemann, P. J., and Jimenez, J. L.: Chemically-resolved aerosol volatility measurements from two megacity field studies, Atmos. Chem. Phys., 9, 7161–7182, doi:10.5194/acp-9-7161-2009, 2009.

Iinuma, Y., Boge, O., Gnauk, T., and Herrmann, H.: Aerosol-chamber study of the alpha-pinene/O-3 reaction: influence of particle acidity on aerosol yields and products, Atmos. Environ., 38, 761–773, 2004.

Iinuma, Y., Boge, O., Miao, Y., Sierau, B., Gnauk, T., and Herrmann, H.: Laboratory studies on secondary organic aerosol formation from terpenes, Faraday Discuss., 130, 279–294, 2005.

Iinuma, Y., Muller, C., Boge, O., Gnauk, T., and Herrmann, H.: The formation of organic sulfate esters in the limonene ozonolysis secondary organic aerosol (SOA) under acidic conditions, Atmos. Environ., 41, 5571–5583, 2007.

Ito, A. and Penner, J. E.: Historical emissions of carbonaceous aerosols from biomass and fossil fuel burning for the period 1870–2000, Global Biogeochem. Cy., 19, GB2028, doi:10.1029/2004GB002374, 2005.

Ito, A., Sillman, S., and Penner, J. E.: Effects of additional nonmethane volatile organic compounds, organic nitrates, and direct emissions of oxygenated organic species on global tropospheric chemistry, J. Geophys. Res., 112, D06309, doi:10.1029/2005JD006556, 2007.

Ito, A., Sillman, S., and Penner, J. E.: Global chemical transport model study of ozone response to changes in chemical kinetics and biogenic volatile organic compounds emissions due to increasing temperatures: Sensitivities to isoprene nitrate chemistry and grid resolution, J. Geophys. Res., 114, D09301, doi:10.1029/2008JD011254, 2009.

Jang, M. S. and Kamens, R. M.: Characterization of secondary aerosol from the photooxidation of toluene in the presence of NO_x and 1-propene, Environ. Sci. Technol., 35, 3626–3639, 2001.

Jang, M. S., Czoschke, N. M., Lee, S., and Kamens, R. M.: Heterogeneous atmospheric aerosol production by acid-catalyzed particle-phase reactions, Science, 298, 814–817, 2002.

Jang, M., Lee, S., and Kamens, R. M.: Organic aerosol growth by acid-catalyzed heterogeneous reactions of octanal in a flow reactor, Atmos. Environ., 37, 2125–2138, 2003a.

Jang, M. S., Carroll, B., Chandramouli, B., and Kamens, R. M.: Particle growth by acid-catalyzed heterogeneous reactions of organic carbonyls on preexisting aerosols, Environ. Sci. Technol., 37, 3828–3837, 2003b.

Jang, M., Czoschke, N. M., and Northcross, A. L.: Atmospheric organic aerosol production by heterogeneous acid-catalyzed reactions, Chemphyschem, 5, 1647–1661, 2004.

Jang, M. S., Czoschke, N. M., and Northcross, A. L.: Semiempirical model for organic aerosol growth by acid-catalyzed heterogeneous reactions of organic carbonyls, Environ. Sci. Technol., 39, 164–174, 2005.

Jang, M., Czoschke, N. M., Northcross, A. L., Cao, G., and Shaof, D.: SOA formation from partitioning and heterogeneous reactions: Model study in the presence of inorganic species, Environ. Sci. Technol., 40, 3013–3022, 2006.

Jimenez, J. L., Canagaratna, M. R., Donahue, N. M., Prevot, A. S. H., Zhang, Q., Kroll, J. H., DeCarlo, P. F., Allan, J. D., Coe, H., Ng, N. L., Aiken, A. C., Docherty, K. S., Ulbrich, I. M., Grieshop, A. P., Robinson, A. L., Duplissy, J., Smith, J. D., Wilson, K. R., Lanz, V. A., Hueglin, C., Sun, Y. L., Tian, J., Laaksonen, A., Raatikainen, T., Rautiainen, J., Vaattovaara, P., Ehn, M., Kulmala, M., Tomlinson, J. M., Collins, D. R., Cubison, M. J., Dunlea, E. J., Huffman, J. A., Onasch, T. B., Alfarra, M. R., Williams, P. I., Bower, K., Kondo, Y., Schneider, J., Drewnick, F., Borrmann, S., Weimer, S., Demerjian, K., Salcedo, D., Cottrell, L., Griffin, R., Takami, A., Miyoshi, T., Hatakeyama, S., Shimono, A., Sun, J. Y., Zhang, Y. M., Dzepina, K., Kimmel, J. R., Sueper, D., Jayne, J. T., Herndon, S. C., Trimborn, A. M., Williams, L. R., Wood, E. C., Middlebrook, A. M., Kolb, C. E., Baltensperger, U., and Worsnop, D. R.: Evolution of Organic Aerosols in the Atmosphere, Science, 326, 1525–1529, 2009.

Johnson, D., Utembe, S. R., and Jenkin, M. E.: Simulating the detailed chemical composition of secondary organic aerosol formed on a regional scale during the TORCH 2003 campaign in the southern UK, Atmos. Chem. Phys., 6, 419–431, doi:10.5194/acp-6-419-2006, 2006.

Kalberer, M., Paulsen, D., Sax, M., Steinbacher, M., Dommen, J., Prevot, A. S. H., Fisseha, R., Weingartner, E., Frankevich, V., Zenobi, R., and Baltensperger, U.: Identification of polymers as major components of atmospheric organic aerosols, Science, 303, 1659–1662, 2004.

Kalberer, M., Sax, M., and Samburova, V.: Molecular size evolution of oligomers in organic aerosols collected in urban atmospheres and generated in a smog chamber, Environ. Sci. Technol., 40, 5917–5922, 2006.

Kamens, R., Jang, M., Chien, C. J., and Leach, K.: Aerosol formation from the reaction of alpha-pinene and ozone using a gas-phase kinetics aerosol partitioning model, Environ. Sci. Technol., 33, 1430–1438, 1999.

Kanakidou, M., Seinfeld, J. H., Pandis, S. N., Barnes, I., Dentener, F. J., Facchini, M. C., Van Dingenen, R., Ervens, B., Nenes, A., Nielsen, C. J., Swietlicki, E., Putaud, J. P., Balkanski, Y., Fuzzi, S., Horth, J., Moortgat, G. K., Winterhalter, R., Myhre, C. E.

L., Tsigaridis, K., Vignati, E., Stephanou, E. G., and Wilson, J.: Organic aerosol and global climate modelling: a review, Atmos. Chem. Phys., 5, 1053–1123, doi:10.5194/acp-5-1053-2005, 2005.

Karl, T., Guenther, A., Turnipseed, A., Tyndall, G., Artaxo, P., and Martin, S.: Rapid formation of isoprene photo-oxidation products observed in Amazonia, Atmos. Chem. Phys., 9, 7753–7767, doi:10.5194/acp-9-7753-2009, 2009.

Karl, T., Harley, P., Emmons, L., Thornton, B., Guenther, A., Basu, C., Turnipseed, A., and Jardine, K.: Efficient atmospheric cleansing of oxidized organic trace gases by vegetation, Science, 330, 816–819, 2010.

Kleindienst, T. E., Jaoui, M., Lewandowski, M., Offenberg, J. H., Lewis, C. W., Bhave, P. V., and Edney, E. O.: Estimates of the contributions of biogenic and anthropogenic hydrocarbons to secondary organic aerosol at a southeastern US location, Atmos. Environ., 41, 8288–8300, 2007.

Kleinman, L. I., Springston, S. R., Daum, P. H., Lee, Y.-N., Nunnermacker, L. J., Senum, G. I., Wang, J., Weinstein-Lloyd, J., Alexander, M. L., Hubbe, J., Ortega, J., Canagaratna, M. R., and Jayne, J.: The time evolution of aerosol composition over the Mexico City plateau, Atmos. Chem. Phys., 8, 1559–1575, doi:10.5194/acp-8-1559-2008, 2008.

Kroll, J. H. and Seinfeld, J. H.: Chemistry of secondary organic aerosol: Formation and evolution of low-volatility organics in the atmosphere, Atmos. Environ., 42, 3593–3624, 2008.

Kroll, J. H., Ng, N. L., Murphy, S. M., Flagan, R. C., and Seinfeld, J. H.: Secondary organic aerosol formation from isoprene photooxidation under high-NO_x conditions, Geophys. Res. Lett., 32, L18808, doi:10.1029/2005GL023637, 2005a.

Kroll, J. H., Ng, N. L., Murphy, S. M., Varutbangkul, V., Flagan, R. C., and Seinfeld, J. H.: Chamber studies of secondary organic aerosol growth by reactive uptake of simple carbonyl compounds, J. Geophys. Res., 110, D23207, doi:10.1029/2005JD006004, 2005b.

Kroll, J. H., Ng, N. L., Murphy, S. M., Flagan, R. C., and Seinfeld, J. H.: Secondary organic aerosol formation from isoprene photooxidation, Environ. Sci. Technol., 40, 1869–1877, 2006.

Kubistin, D., Harder, H., Martinez, M., Rudolf, M., Sander, R., Bozem, H., Eerdekens, G., Fischer, H., Gurk, C., Klüpfel, T., Königstedt, R., Parchatka, U., Schiller, C. L., Stickler, A., Taraborrelli, D., Williams, J., and Lelieveld, J.: Hydroxyl radicals in the tropical troposphere over the Suriname rainforest: comparison of measurements with the box model MECCA, Atmos. Chem. Phys., 10, 9705–9728, doi:10.5194/acp-10-9705-2010, 2010.

Lee-Taylor, J., Madronich, S., Aumont, B., Baker, A., Camredon, M., Hodzic, A., Tyndall, G. S., Apel, E., and Zaveri, R. A.: Explicit modeling of organic chemistry and secondary organic aerosol partitioning for Mexico City and its outflow plume, Atmos. Chem. Phys., 11, 13219–13241, doi:10.5194/acp-11-13219-2011, 2011.

Lelieveld, J., Butler, T. M., Crowley, J. N., Dillon, T. J., Fischer, H., Ganzeveld, L., Harder, H., Lawrence, M. G., Martinez, M., Taraborrelli, D., and Williams, J.: Atmospheric oxidation capacity sustained by a tropical forest, Nature, 452, 737–740, 2008.

Lewis, C. W., Klouda, G. A., and Ellenson, W. D.: Radiocarbon measurement of the biogenic contribution to summertime PM-2.5 ambient aerosol in Nashville, TN, Atmos. Environ., 38, 6053–6061, 2004.

Liao, H., Henze, D. K., Seinfeld, J. H., Wu, S. L., and Mickley, L. J.: Biogenic secondary organic aerosol over the United States: Comparison of climatological simulations with observations, J. Geophys. Res., 112, D06201, doi:10.1029/2006JD007813, 2007.

Liggio, J., Li, S. M., and McLaren, R.: Reactive uptake of glyoxal by particulate matter, J. Geophys. Res., 110, D10304, doi:10.1029/2004JD005113, 2005a.

Liggio, J., Li, S. M., and McLaren, R.: Heterogeneous reactions of glyoxal on particulate matter: Identification of acetals and sulfate esters, Environ. Sci. Technol., 39, 1532-1541, 2005b.

Lim, Y. B., Tan, Y., Perri, M. J., Seitzinger, S. P., and Turpin, B. J.: Aqueous chemistry and its role in secondary organic aerosol (SOA) formation, Atmos. Chem. Phys., 10, 10521–10539, doi:10.5194/acp-10-10521-2010, 2010.

Liu, X. H. and Penner, J. E.: Effect of Mount Pinatubo H_2SO_4/H_2O aerosol on ice nucleation in the upper troposphere using a global chemistry and transport model, J. Geophys. Res., 107, D12, doi:10.1029/2001JD000455, 2002.

Liu, H. Y., Jacob, D. J., Bey, I., and Yantosca, R. M.: Constraints from Pb-210 and Be-7 on wet deposition and transport in a global three-dimensional chemical tracer model driven by assimilated meteorological fields, J. Geophys. Res., 106, 12109–12128, 2001.

Liu, X. H., Penner, J. E., and Herzog, M.: Global modeling of aerosol dynamics: Model description, evaluation, and interactions between sulfate and nonsulfate aerosols, J. Geophys. Res., 110, D18206, doi:10.1029/2004JD005674, 2005.

Loeffler, K. W., Koehler, C. A., Paul, N. M., and De Haan, D. O.: Oligomer formation in evaporating aqueous glyoxal and methylglyoxal solutions, Environ. Sci. Technol., 40, 6318–6323, 2006.

Luo, G. and Yu, F.: A numerical evaluation of global oceanic emissions of α-pinene and isoprene, Atmos. Chem. Phys., 10, 2007–2015, doi:10.5194/acp-10-2007-2010, 2010.

Malm, W. C., Pitchford, M. L., Scuggs, M., Sisler, J. F., Ames, R., Copeland, S., Gebhart, K. A., and Day, D. E.: Spatial and seasonal patterns and temporal variability of haze and its constituents in the United States, Rep. III, Coop. Inst. for Res., Colo. State Univ., Fort Collins, 2000.

Mari, C., Jacob, D. J., and Bechtold, P.: Transport and scavenging of soluble gases in a deep convective cloud, J. Geophys. Res., 105, 22255–22267, 2000.

Maria, S. F., Russell, L. M., Turpin, B. J., Porcja, R. J., Campos, T. L., Weber, R. J., and Huebert, B. J.: Source signatures of carbon monoxide and organic functional groups in Asian Pacific Regional Aerosol Characterization Experiment (ACE-Asia) submicron aerosol types, J. Geophys. Res., 108, D23, doi:10.1029/2003JD003703, 2003.

Martinez, M., Harder, H., Kubistin, D., Rudolf, M., Bozem, H., Eerdekens, G., Fischer, H., Klüpfel, T., Gurk, C., Königstedt, R., Parchatka, U., Schiller, C. L., Stickler, A., Williams, J., and Lelieveld, J.: Hydroxyl radicals in the tropical troposphere over the Suriname rainforest: airborne measurements, Atmos. Chem. Phys., 10, 3759–3773, doi:10.5194/acp-10-3759-2010, 2010.

Minerath, E. C. and Elrod, M. J.: Assessing the potential for diol and hydroxy sulfate ester formation from the reaction of epoxides in tropospheric aerosols, Environ. Sci. Technol., 43, 1386–1392, 2009.

Minerath, E. C., Schultz, M. P., and Elrod, M. J.: Kinetics of the reactions of isoprene-derived epoxides in model tropospheric aerosol solutions, Environ. Sci. Technol., 43, 8133–8139, 2009.

Myrdal, P. B. and Yalkowsky, S. H.: Estimating pure component vapor pressures of complex organic molecules, Industrial & Engineering Chemistry Research, 36, 2494–2499, 1997.

Nannoolal, Y., Rarey, J., and Ramjugernath, D.: Estimation of pure component properties, Part 3, Estimation of the vapor pressure of non-electrolyte organic compounds via group contributions and group interactions, Fluid Phase Equilibr., 269, 117–133, 2008

Ng, N. L., Kroll, J. H., Keywood, M. D., Bahreini, R., Varutbangkul, V., Flagan, R. C., Seinfeld, J. H., Lee, A., and Goldstein, A. H.: Contribution of first- versus second-generation products to secondary organic aerosols formed in the oxidation of biogenic hydrocarbons, Environ. Sci. Technol., 40, 2283–2297, 2006.

Ng, N. L., Chhabra, P. S., Chan, A. W. H., Surratt, J. D., Kroll, J. H., Kwan, A. J., McCabe, D. C., Wennberg, P. O., Sorooshian, A., Murphy, S. M., Dalleska, N. F., Flagan, R. C., and Seinfeld, J. H.: Effect of NO_x level on secondary organic aerosol (SOA) formation from the photooxidation of terpenes, Atmos. Chem. Phys., 7, 5159–5174, doi:10.5194/acp-7-5159-2007, 2007.

Nozière, B., González, N. J. D., Borg-Karlson, A.-K., Pei, Y., Redeby, J. P., Krejci, R., Dommen, J., Prevot, A. S. H., and Anthonsen, T.: Atmospheric chemistry in stereo: A new look at secondary organic aerosols from isoprene, Geophys. Res. Lett., 38, L11807, doi:10.1029/2011GL047323, 2011.

Odum, J. R., Hoffmann, T., Bowman, F., Collins, D., Flagan, R. C., and Seinfeld, J. H.: Gas/particle partitioning and secondary organic aerosol yields, Environ. Sci. Technol., 30, 2580–2585, 1996.

O'Donnell, D., Tsigaridis, K., and Feichter, J.: Estimating the direct and indirect effects of secondary organic aerosols using ECHAM5-HAM, Atmos. Chem. Phys., 11, 8635–8659, doi:10.5194/acp-11-8635-2011, 2011.

O'Dowd, C. D., Langmann, B., Varghese, S., Scannell, C., Ceburnis, D., and Facchini, M. C.: A combined organic-inorganicsea-spray source function, Geophys. Res. Let., 35, L01801, doi:10.1029/2007GL030331, 2008.

Palmer, P. I. and Shaw, S. L.: Quantifying global marine isoprene fluxes using MODIS chlorophyll observations, Geophys. Res. Lett., 32, L09805, doi:10.1029/2005GL022592, 2005.

Pankow, J. F.: An absorption-model of the gas aerosol partitioning involved in the formation of secondary organic aerosol, Atmos. Environ., 28, 189–193, 1994.

Pankow, J. F. and Asher, W. E.: SIMPOL.1: a simple group contribution method for predicting vapor pressures and enthalpies of vaporization of multifunctional organic compounds, Atmos. Chem. Phys., 8, 2773–2796, doi:10.5194/acp-8-2773-2008, 2008.

Pankow, J. F. and Barsanti, K. C.: The carbon number-polarity grid: A means to manage the complexity of the mix of organic compounds when modeling atmospheric organic particulate matter, Atmos. Environ., 43, 2829–2835, 2009.

Park, R. J., Jacob, D. J., Chin, M., and Martin, R. V.: Sources ofcarbonaceous aerosols over the United States and implications fornatural visibility, J. Geophys. Res., 108, 4355, doi:10.1029/2002JD003190, 2003.

Paulot, F., Crounse, J. D., Kjaergaard, H. G., Kurten, A., St Clair, J. M., Seinfeld, J. H., and Wennberg, P. O.: Unexpected epoxide formation in the gas-phase photooxidation of isoprene, Science, 325, 730–733, 2009.

Paulsen, D., Weingartner, E., Alfarra, M. R., and Baltensperger, U.: Volatility measurements of photochemically and nebulizer-generated organic aerosol particles, J. Aerosol Sci., 37, 1025–1051, 2006.

Peeters, J. and Müller, J.-F.: HO_x radical regeneration in isoprene oxidation via peroxy radical isomerisations. II: experimental evidence and global impact, Phys. Chem. Chem. Phys., 12, 14227–14235, 2010.

Peeters, J., Nguyen, T. L., and Vereecken, L.: HO_x radical regeneration in the oxidation of isoprene, Phys. Chem. Chem. Phys., 11, 5935–5939, 2009.

Penner, J. E., Chuang, C. C., and Grant, K.: Climate forcing by carbonaceous and sulfate aerosols, Clim. Dynam., 14, 839–851, 1998.

Perraud, V., Bruns, E. A., Eznll, M. J., Johnson, S. N., Yu, Y., Alexander, M. L., Zelenyuk, A., Imre, D., Chang, W. L., Dabdub, D., Pankow, J. F., and Finlayson-Pitts, B. J.: Nonequilibrium atmospheric secondary organic aerosol formation and growth, P. Natl. Acad. Sci. USA, 109, 2836–2841, 2012.

Pugh, T. A. M., MacKenzie, A. R., Hewitt, C. N., Langford, B., Edwards, P. M., Furneaux, K. L., Heard, D. E., Hopkins, J. R., Jones, C. E., Karunaharan, A., Lee, J., Mills, G., Misztal, P., Moller, S., Monks, P. S., and Whalley, L. K.: Simulating atmospheric composition over a South-East Asian tropical rainforest: performance of a chemistry box model, Atmos. Chem. Phys., 10, 279–298, doi:10.5194/acp-10-279-2010, 2010.

Pun, B. K., Seigneur, C., and Lohman, K.: Modeling secondary organic aerosol formation via multiphase partitioning with molecular data, Environ. Sci. Technol., 40, 4722–4731, 2006.

Pye, H. O. T. and Seinfeld, J. H.: A global perspective on aerosol from low-volatility organic compounds, Atmos. Chem. Phys., 10, 4377–4401, doi:10.5194/acp-10-4377-2010, 2010.

Reid, R. C., Prausnitz, J. M., and Polling, B. E.: The properties of gases and liquids, Hill, New York, USA, 1987.

Robinson, A. L., Donahue, N. M., Shrivastava, M. K., Weitkamp, E. A., Sage, A. M., Grieshop, A. P., Lane, T. E., Pierce, J. R., and Pandis, S. N.: Rethinking organic aerosols: Semivolatile emissions and photochemical aging, Science, 315, 1259–1262, 2007.

Robinson, N. H., Hamilton, J. F., Allan, J. D., Langford, B., Oram, D. E., Chen, Q., Docherty, K., Farmer, D. K., Jimenez, J. L., Ward, M. W., Hewitt, C. N., Barley, M. H., Jenkin, M. E., Rickard, A. R., Martin, S. T., McFiggans, G., and Coe, H.: Evidence for a significant proportion of Secondary Organic Aerosol from isoprene above a maritime tropical forest, Atmos. Chem. Phys., 11, 1039–1050, doi:10.5194/acp-11-1039-2011, 2011.

Rotman, D. A., Atherton, C. S., Bergmann, D. J., Cameron-Smith, P. J., Chuang, C. C., Connell, P. S., Dignon, J. E., Franz, A., Grant, K. E., Kinnison, D. E., Molenkamp, C. R., Proctor, D. D., and Tannahill, J. R.: IMPACT, the LLNL 3-D global atmospheric chemical transport model for the combined troposphere and stratosphere: Model description and analysis of ozone and other trace gases, J. Geophys. Res., 109, D04303, doi:10.1029/2002JD003155, 2004.

Saathoff, H., Naumann, K.-H., Möhler, O., Jonsson, Å. M., Hallquist, M., Kiendler-Scharr, A., Mentel, Th. F., Tillmann, R., and Schurath, U.: Temperature dependence of yields of secondary organic aerosols from the ozonolysis of α-pinene and limonene,

Atmos. Chem. Phys., 9, 1551–1577, doi:10.5194/acp-9-1551-2009, 2009.

Sato, K., Hatakeyama, S., and Imamura, T.: Secondary organic aerosol formation during the photooxidation of toluene: NO_x dependence of chemical composition, J. Phys. Chem. A, 111, 9796–9808, 2007.

Seinfeld, J. H. and Pandis, S. N.: Atmospheric chemistry and physics: from air pollution to climate change, John Wiley, Hoboken, N. J., 1998.

Sillman, S.: A numerical-solution for the equations of tropospheric chemistry based on an analysis of sources and sinks of odd hydrogen, J. Geophys. Res., 96, 20735–20744, 1991.

Simpson, D., Yttri, K. E., Klimont, Z., Kupiainen, K., Caseiro, A., Gelencsér, A., Pio, C., Puxbaum, H., and Legrand, M.: Modeling carbonaceous aerosol over Europe: Analysis of the CARBOSOL and EMEP EC/OC campaigns, J. Geophys. Res., 112, D23S14, doi:10.1029/2006JD008158, 2007.

Slowik, J. G., Stroud, C., Bottenheim, J. W., Brickell, P. C., Chang, R. Y.-W., Liggio, J., Makar, P. A., Martin, R. V., Moran, M. D., Shantz, N. C., Sjostedt, S. J., van Donkelaar, A., Vlasenko, A., Wiebe, H. A., Xia, A. G., Zhang, J., Leaitch, W. R., and Abbatt, J. P. D.: Characterization of a large biogenic secondary organic aerosol event from eastern Canadian forests, Atmos. Chem. Phys., 10, 2825–2845, doi:10.5194/acp-10-2825-2010, 2010.

Song, C., Zaveri, R. A., Alexander, M. L., Thornton, J. A., Madronich, S., Ortega, J. V., Zelenyuk, A., Yu, X. Y., Laskin, A., and Maughan, D. A.: Effect of hydrophobic primary organic aerosols on secondary organic aerosol formation from ozonolysis of alpha-pinene, Geophys. Res. Lett., 34, L20803, doi:10.1029/2007GL030720, 2007.

Spracklen, D. V., Jimenez, J. L., Carslaw, K. S., Worsnop, D. R., Evans, M. J., Mann, G. W., Zhang, Q., Canagaratna, M. R., Allan, J., Coe, H., McFiggans, G., Rap, A., and Forster, P.: Aerosol mass spectrometer constraint on the global secondary organic aerosol budget, Atmos. Chem. Phys., 11, 12109–12136, doi:10.5194/acp-11-12109-2011, 2011.

Stanier, C. O., Pathak, R. K., and Pandis, S. N.: Measurements of the volatility of aerosols from alpha-piniene ozonolysis, Environ. Sci. Technol., 41, 2756–2763, 2007.

Stavrakou, T., Müller, J.-F., De Smedt, I., Van Roozendael, M., Kanakidou, M., Vrekoussis, M., Wittrock, F., Richter, A., and Burrows, J. P.: The continental source of glyoxal estimated by the synergistic use of spaceborne measurements and inverse modelling, Atmos. Chem. Phys., 9, 8431–8446, doi:10.5194/acp-9-8431-2009, 2009.

Stavrakou, T., Peeters, J., and Müller, J.-F.: Improved global modelling of HO_x recycling in isoprene oxidation: evaluation against the GABRIEL and INTEX-A aircraft campaign measurements, Atmos. Chem. Phys., 10, 9863–9878, doi:10.5194/acp-10-9863-2010, 2010.

Stone, D., Evans, M. J., Commane, R., Ingham, T., Floquet, C. F. A., McQuaid, J. B., Brookes, D. M., Monks, P. S., Purvis, R., Hamilton, J. F., Hopkins, J., Lee, J., Lewis, A. C., Stewart, D., Murphy, J. G., Mills, G., Oram, D., Reeves, C. E., and Heard, D. E.: HO_x observations over West Africa during AMMA: impact of isoprene and NO_x, Atmos. Chem. Phys., 10, 9415–9429, doi:10.5194/acp-10-9415-2010, 2010.

Stroud, C. A., Makar, P. A., Moran, M. D., Gong, W., Gong, S., Zhang, J., Hayden, K., Mihele, C., Brook, J. R., Abbatt, J. P. D., and Slowik, J. G.: Impact of model grid spacing on regional- and urban- scale air quality predictions of organic aerosol, Atmos. Chem. Phys., 11, 3107–3118, doi:10.5194/acp-11-3107-2011, 2011.

Surratt, J. D., Lewandowski, M., Offenberg, J. H., Jaoui, M., Kleindienst, T. E., Edney, E. O., and Seinfeld, J. H.: Effect of acidity on secondary organic aerosol formation from isoprene, Environ. Sci. Technol., 41, 5363–5369, 2007.

Surratt, J. D., Chan, A. W. H., Eddingsaas, N. C., Chan, M. N., Loza, C. L., Kwan, A. J., Hersey, S. P., Flagan, R. C., Wennberg, P. O., and Seinfeld, J. H.: Reactive intermediates revealed in secondary organic aerosol formation from isoprene, P. Natl. Acad. Sci. USA, 107, 6640–6645, 2010.

Szidat, S., Prévôt, A. S. H., Sandradewi, J., Alfarra, M. R., Synal, H.-A., Wacker, L., and Baltensperger, U.: Dominant impact of residential wood burning on particulate matter in Alpine valleys during winter, Geophys. Res. Lett., 34, L05820, doi:10.1029/2006GL028325, 2007.

Szidat, S., Ruff, M., Perron, N., Wacker, L., Synal, H.-A., Hallquist, M., Shannigrahi, A. S., Yttri, K. E., Dye, C., and Simpson, D.: Fossil and non-fossil sources of organic carbon (OC) and elemental carbon (EC) in Göteborg, Sweden, Atmos. Chem. Phys., 9, 1521–1535, doi:10.5194/acp-9-1521-2009, 2009.

Tan, Y., Carlton, A. G., Seitzinger, S. P., and Turpin, B. J.: SOA from methylglyoxal in clouds and wet aerosols: Measurement and prediction of key products, Atmos. Environ., 44, 5218–5226, 2010.

Tsigaridis, K. and Kanakidou, M.: Global modelling of secondary organic aerosol in the troposphere: a sensitivity analysis, Atmos. Chem. Phys., 3, 1849–1869, doi:10.5194/acp-3-1849-2003, 2003.

Tsigaridis, K. and Kanakidou, M.: Secondary organic aerosol importance in the future atmosphere, Atmos. Environ., 41, 4682–4692, 2007.

Tsigaridis, K., Krol, M., Dentener, F. J., Balkanski, Y., Lathière, J., Metzger, S., Hauglustaine, D. A., and Kanakidou, M.: Change in global aerosol composition since preindustrial times, Atmos. Chem. Phys., 6, 5143–5162, doi:10.5194/acp-6-5143-2006, 2006.

Trainic, M., Abo Riziq, A., Lavi, A., Flores, J. M., and Rudich, Y.: The optical, physical and chemical properties of the products of glyoxal uptake on ammonium sulfate seed aerosols, Atmos. Chem. Phys., 11, 9697–9707, doi:10.5194/acp-11-9697-2011, 2011.

Utembe, S. R., Cooke, M. C., Archibald, A. T., Shallcross, D. E., Derwent, R. G., and Jenkin, M. E.: Simulating secondary organic aerosol in a 3-D Lagrangian chemistry transport model using the reduced Common Representative Intermediates mechanism (CRI v2-R5), Atmos. Environ., 45, 1604–1614, 2011.

Vaden, T. D., Imre, D., Beranek, J., Shrivastava, M., and Zelenyuk, A.: Evaporation kinetics and phase of laboratory and ambient secondary organic aerosol, P. Natl. Acad. Sci. USA, 108, 2190–2195, 2011.

Valorso, R., Aumont, B., Camredon, M., Raventos-Duran, T., Mouchel-Vallon, C., Ng, N. L., Seinfeld, J. H., Lee-Taylor, J., and Madronich, S.: Explicit modelling of SOA formation from α-pinene photooxidation: sensitivity to vapour pressure estimation, Atmos. Chem. Phys., 11, 6895–6910, doi:10.5194/acp-11-6895-2011, 2011.

Volkamer, R., Jimenez, J. L., San Martini, F., Dzepina, K., Zhang, Q., Salcedo, D., Molina, L. T., Worsnop, D. R., and Molina, M. J.: Secondary organic aerosol formation from anthropogenic air pollution: Rapid and higher than expected, Geophys. Res. Lett., 33, L17811, doi:10.1029/2006GL026899, 2006.

Volkamer, R., Martini, F. S., Molina, L. T., Salcedo, D., Jimenez, J. L., and Molina, M. J.: A missing sink for gas-phase glyoxal in Mexico City: Formation of secondary organic aerosol, Geophys. Res. Lett., 34, L19807, doi:10.1029/2007GL030752, 2007.

Volkamer, R., Ziemann, P. J., and Molina, M. J.: Secondary Organic Aerosol Formation from Acetylene (C_2H_2): seed effect on SOA yields due to organic photochemistry in the aerosol aqueous phase, Atmos. Chem. Phys., 9, 1907–1928, doi:10.5194/acp-9-1907-2009, 2009.

Wang, M. and Penner, J. E.: Aerosol indirect forcing in a global model with particle nucleation, Atmos. Chem. Phys., 9, 239–260, doi:10.5194/acp-9-239-2009, 2009.

Wang, M. H., Penner, J. E., and Liu, X. H.: Coupled IMPACT aerosol and NCAR CAM3 model: Evaluation of predicted aerosol number and size distribution, J. Geophys. Res., 114, D06302, doi:10.1029/2008JD010459, 2009.

Wang, Y. H., Jacob, D. J., and Logan, J. A.: Global simulation of tropospheric O-3-NO_x-hydrocarbon chemistry 1. Model formulation, J. Geophys. Res., 103, 10713–10725, 1998.

Wesely, M. L.: Parameterization of surface resistances to gaseous dry deposition in regional-scale numerical models, Atmos. Environ., 23, 1293–1304, 1989.

Xia, A. G., Michelangeli, D. V., and Makar, P. A.: Box model studies of the secondary organic aerosol formation under different HC/NO_x conditions using the subset of the Master Chemical Mechanism for alpha-pinene oxidation, J. Geophys. Res., 113, D10301, doi:10.1029/2007JD008726, 2008.

Yoon, Y. J., Ceburnis, D., Cavalli, F., Jourdan, O., Putaud, J. P., Facchini, M. C., Decesari, S., Fuzzi, S., Sellegri, K., Jennings, S. G., and O'Dowd, C. D.: Seasonal characteristics of the physicochemical properties of North Atlantic marine atmospheric aerosols, J. Geophys. Res., 112, D04206, doi:10.1029/2005JD007044, 2007.

Yttri, K. E., Aas, W., Bjerke, A., Cape, J. N., Cavalli, F., Ceburnis, D., Dye, C., Emblico, L., Facchini, M. C., Forster, C., Hanssen, J. E., Hansson, H. C., Jennings, S. G., Maenhaut, W., Putaud, J. P., and Tørseth, K.: Elemental and organic carbon in PM_{10}: a one year measurement campaign within the European Monitoring and Evaluation Programme EMEP, Atmos. Chem. Phys., 7, 5711–5725, doi:10.5194/acp-7-5711-2007, 2007.

Yu, F.: A secondary organic aerosol formation model considering successive oxidation aging and kinetic condensation of organic compounds: global scale implications, Atmos. Chem. Phys., 11, 1083–1099, doi:10.5194/acp-11-1083-2011, 2011.

Zhang, J. Y., Huff Hartz, K. E., Pandis S. N., and Donahue, N. M.: Secondary organic aerosol formation from limonene ozonolysis: Homogeneous and heterogeneous influences as a function of NO_x, J. Phys. Chem. A, 110, 11053–11063, 2006.

Zhang, Q., Jimenez, J. L., Canagaratna, M. R., Allan, J. D., Coe, H., Ulbrich, I., Alfarra, M. R., Takami, A., Middlebrook, A. M., Sun, Y. L., Dzepina, K., Dunlea, E., Docherty, K., DeCarlo, P. F., Salcedo, D., Onasch, T., Jayne, J. T., Miyoshi, T., Shimono, A., Hatakeyama, S., Takegawa, N., Kondo, Y., Schneider, J., Drewnick, F., Borrmann, S., Weimer, S., Demerjian, K., Williams, P., Bower, K., Bahreini, R., Cottrell, L., Griffin, R. J., Rautiainen, J., Sun, J. Y., Zhang, Y. M., and Worsnop, D. R.: Ubiquity and dominance of oxygenated species in organic aerosols in anthropogenically-influenced Northern Hemisphere midlatitudes, Geophys. Res. Lett., 34, L13801, doi:10.1029/2007GL029979, 2007.

Zhang, S., Penner, J. E., and Torres, O.: Inverse modeling of biomass burning emissions using total ozone mapping spectrometer aerosol index for 1997, J. Geophys. Res., 110, D21306, doi:10.1029/2004JD005738, 2005.

Zhang, Y., Pun, B., Vijayaraghavan, K., Wu, S. Y., Seigneur, C., Pandis, S. N., Jacobson, M. Z., Nenes, A., and Seinfeld, J. H.: Development and application of the model of aerosol dynamics, reaction, ionization, and dissolution (MADRID), J. Geophys. Res., 109, D01202, doi:10.1029/2003JD003501, 2004.